

INTERFERENCE PATTERN CALCULATION  
OF SPACE WAVE PROPAGATION FOR  
MICROWAVE COMMUNICATION LINKS

A Thesis

by

Sunil Kumar Adhikary

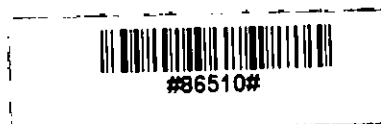
Submitted to the Department of Electrical and Electronic  
Engineering of Bangladesh University of Engineering and  
Technology Dhaka in partial fulfilment of the requirements for  
the degree of

MASTER OF SCIENCE IN ENGINEERING (Electrical and Electronic)



Department of Electrical and Electronic Engineering  
Bangladesh University of Engineering and Technology, Dhaka-1000

June 1993



"R"  
623.849  
1993  
ADH

The thesis titled "INTERFERENCE PATTERN CALCULATION OF SPACE WAVE PROPAGATION FOR MICROWAVE COMMUNICATION LINKS" submitted by Sunil Kumar Adhikary, Roll No.901304F, Session '88-89 to the Department of Electrical and Electronic Engineering of B.U.E.T. has been accepted as satisfactory in partial fulfilment of the requirements for the degree of Master of Science in Engineering (Electrical and Electronic).

Examination held on : 17 June 1993.

Board of Examiners

1. *Abdul Siddique Hossain*  
.....  
Dr. A. B. M. Siddique Hossain  
Professor  
Department of EEE  
B. U. E. T., Dhaka-1000  
Chairman  
(Supervisor)
2. *Saiful Islam*  
..... 17.6.93  
Dr. Saiful Islam  
Professor and Head  
Department of EEE  
B. U. E. T., Dhaka-1000  
Member  
(Ex-officio)
3. *M. A. Matin*  
..... 17.6.93  
Dr. Md. Abdul Matin  
Professor  
Department of EEE  
B. U. E. T., Dhaka-1000  
Member
4. *Shmed*  
.....  
Prof. Dr. Shamsuddin Ahmed  
Head  
Department of EEE  
ICTVTR, Board Bazar, Gazipur  
Member  
(External)

## Declaration

I hereby declare that this work has been done by me and it has not been submitted elsewhere for the award of any degree or diploma.

Countersigned

Abdul Siddique Hossain 17/06/93  
(Dr. A.B.M. Siddique Hossain)

Signature of the student

Sunil Kumar Adhikary 17-6-93  
(Sunil Kumar Adhikary)

## Acknowledgement

The author acknowledges thanks to a number of persons who have helped so much in compiling this thesis work.

The author is indebted to Dr. A. B. M. Siddique Hossain, Professor and Dean, Faculty of Electrical and Electronic Engg., BUET for his dynamic guidance and helpful suggestions. The thesis work has been completed under his supervision. His keen interest and sincerity have made it possible to complete the thesis work. The author expresses his sincere and heartfelt gratitude to him.

The author thankfully acknowledges the valuable discussions occasionally made with Dr. Saiful Islam, Professor and Head, Department of Electrical and Electronic Engineering, BUET and for his sincere help toward the progress of this work.

The author is also grateful to Mr. Mazed Sarker, Divisional Engineer(MW1) of Bangladesh Telegraph & Telephone Board for his helpful counsel and guidance.

The author expresses his grateful acknowledgement and indebtedness to the engineers of Bangladesh Telephone & Telegraph Board for their help in providing relevant data.

The author is thankful to Mr. Subhangker Pandit and Miss Malobica Sarker Shilpi for their encouragement to complete the work successfully.

# Contents

	<u>Page</u>
A. Declaration	ii
B. Acknowledgement	iii
C. Contents	iv
D. List of figures	viii
E. List of Symbols	xi
F. Abstract	xv
 <u>CHAPTER 1</u>	
<u>Introduction</u>	01
1.1 Propagation of electromagnetic waves and interference effect.	01
1.2 Propagation due to frequency range	04
1.3 Frequency Band Designation	06
 <u>CHAPTER 2</u>	
<u>Radio wave interference phenomena over flat earth</u>	07
2.1 Introduction	07
2.2 General features of interference phenomena with antennas located over a flat earth	07
2.3 Reflection co-efficient for propagation	11
2.4 Patterns of coverage diagram	17
2.5 Effect of roughness in propagation	21
2.6 Variation of space wave field strength with distance	22

	<u>Page</u>
<u>CHAPTER 3</u>	
<u>Radio wave propagation phenomena over spherical earth</u>	25
3.1 Effect of curvature of earth in propagation and atmospheric effects	25
3.2 Mathematical analysis for effective earth radius	28
3.3 Range of space wave propagation	31
3.4 General feature of interference phenomena with antennas located over spherical earth	33
3.5 Patterns of coverage diagram	38
3.6 The field in the diffraction zone	45
3.7 Midpath obstacle diffraction loss	48
 <u>CHAPTER 4</u>	
<u>Microwave Communication link performance Calculation</u>	54
4.1 System link model	54
4.2 Radio system performance calculation	54
4.3 Noise requirement	56
4.3.1 Thermal noise	56
4.3.2 Quantum noise	58
4.3.3 Intermodulation noise	58
4.3.4 Cross talk noise	58
4.3.5 Impulse noise	59
4.3.6 Signal to noise ratio (S/N)	59

	<u>Page</u>
4.4 Noise figure and noise temperature	60
4.5 Required received carrier level	62
4.6 Link equation and system gain	63
4.7 Unfaded interference noise (S/I) calculation	66
4.8 Fade margin requirements for a specified system availability	67

## CHAPTER 5

### Calculation for a microwave link in Bangladesh

5.1 Introduction	70
5.2 Calculation of an UHF link	70
5.2.1 Datas and parameters	70
5.2.2 Patterns of coverage diagram	70
5.2.3 Fresnel zone calculation	71
5.2.4 Performance calculation	71
5.3 Calculation for a SHF link (Manikganj-Dhaka radio link)	72
5.3.1 Hop characteristics	72
5.3.2 Station parameters	72
5.3.3 Results	73
5.4 Discussion	73

## CHAPTER 6

### Conclusions

6.1 Summary	82
-------------	----

	<u>Page</u>
6.2 Suggestions for future work	82
 <u>Appendices</u>	
Appendix A. Microwave frequency band designation	85
Appendix B. Calculation of (Effective earth correction factor) constant k	86
Appendix C. Listing of computer programs	89
 <u>References</u>	 93



## List of figures

<u>Figure number</u>	<u>Title</u>	<u>Page</u>
1.1	Illustration of propagation paths	02
2.1	Illustration of direct and reflected rays	09
2.2	Illustration of elevation angle	09
2.3	Phasor diagram of resultant field strength	13
2.4	Magnitude and phase of reflection coefficient for horizontal polarization ( $\sigma=12 \times 10^{-3}$ , $\epsilon_1=15$ )	13
2.5	Magnitude and phase of reflection coefficient for vertical polarization ( $\sigma=12 \times 10^{-3}$ , $\epsilon_1=15$ )	14
2.6	Magnitude of the reflection coefficient for $\epsilon_1=10$ .	15
2.7	Phase of the reflection coefficient for $\epsilon_1=10$ .	16
2.8	Coverage diagram (Flat earth approximation) for $h_1=800\lambda_0$ , $r_f=20\text{km}$ .	19
2.9	Coverage diagram (Flat earth approximation) for $h_1=1625\lambda_0$ , $r_f=22.15\text{km}$ .	20
2.10	A typical plot of field strength against distance from transmitter	24
3.1	Illustration of radio horizon and optical horizon	27
3.2	Illustration of ray curvature	27
3.3	Illustration of reflection of tropospheric wave	30
3.4	Equivalent ray paths over earth (a) True radius 'a' and (b) Modified radius $a_e$ .	30
3.5	Illustration of horizontal range	34
3.6	Illustration of reflection from a spherical earth	34

<u>Figure number</u>	<u>Title</u>	<u>Page</u>
3.7	Illustration of ray divergence upon reflection from a spherical surface	37
3.8	Illustration of constant height curve	37
3.9	Contours showing constant values of divergence factor $D$ and the path divergence phase variable (a) Contours for the value of $h_2/h_1$ up to 4. (b) Contours for the value of $h_2/h_1$ up to 50.	40
3.10	Data for constructing a coverage diagram for $v=0.268$ .	43
3.11	Coverage diagram for $v=0.268$ based on data in figure 3.10	44
3.12	A typical plot of attenuation function $V(X)$ (in dB) against distance $(X)$	46
3.13	Illustration of the height gain function $V(Z)$	46
3.14	Path gain factor $F$ in dB for $h_1=25m$ , $h_2=60m$ and $f=3GHz$	49
3.15	Illustration of midpath obstacle	49
3.16(a)	Knife-edge model (b) Knife-edge model showing propagation parameters.	50
3.17	Illustration of first Fresnel zone	52
3.18	The path gain factor $F_d$ caused by knife-edge diffraction loss in dB as a function of $H_c$	52
4.1	A microwave link model	55
4.2	A resistor connected to a passive network	55
4.3	Illustration of cross talk noise	61
4.4	Equivalent noisy transducer	61
5.1	Coverage diagram (Flat earth approximation) for an UHF link ( $h_1=300\lambda_0$ , $r_f=12.5km$ )	75

<u>Figure number</u>	<u>Title</u>	<u>Page</u>
5.2	Coverage diagram (Spherical earth approximation) for an UHF link ( $v = 0.57$ )	76
5.3	First Fresnel zone for a UHF link ( $f=1.5$ GHz, $d=25.00$ km, $k=1.33$ , $h_1=24.5$ m, $h_2=60$ m)	76
5.4	Coverage diagram for an UHF link ( $h_1=300\lambda_0$ , $r_f=15$ Km )	77
5.5	Coverage diagram for Manikganj -Dhaka MW link (Flat -earth ) for $h_1=86$ m, $f=6.77$ GHz, $r_f=22.15$ km.	78
5.6	Data for constructing coverage diagram for M.ganj-Dhaka MW link (Spherical earth) for $v = 10.956$ .	79
5.7	Magnitude and phase of reflection co-efficient for horizontal polarization in 3-12 GHz range ( $\epsilon = 15.00$ , $\sigma = 0.009$ )	80
5.8	Magnitude and phase of reflection co-efficient for vertical polarization in 3-12 GHz range ( $\epsilon = 15.00$ , $\sigma = 0.009$ )	81
6.1	Attenuation by oxygen and water vapor at sea level. $T = 20^{\circ}$ C.	84

## List of symbols

<u>Symbols</u>	<u>Description</u>
$f_1$	Radiation field strength pattern of transmitting antenna
$f_2$	Radiation field strength pattern of receiving antenna
$h_1$	Transmitting antenna height
$h_2$	Receiving antenna height
$k_0$	Propagation constant
$\rho e^{j\phi}$	Reflection co-efficient
$\rho$	Magnitude of reflection co-efficient
$\phi/\phi_v$	Phase angle of reflection co-efficient /Vertical polarization/Horizontal polarization
$R_1$	Direct path length
$R_2$	Reflected path length
$\psi$	Grazing angle
$\psi_0$	Elevation angle
$F$	Path gain factor
$\lambda_0$	Wave length
$\sigma$	Ground conductivity
$k$	Dielectric constant
$f$	Frequency
$r_f$	Free space reference range
$r$	Direct line-of-sight length (Chapter 2)
$\epsilon$	Permittivity

<u>Symbols</u>	<u>Description</u>
$v$	Vertical direction wave length
$N$	Refractivity
$n$	Refractive index
$p$	Pressure
$e$	Partial pressure of water vapor
$T$	Ratio of antenna heights (Chapter 3)
$T$	Absolute Temperature (Chapter 4)
$D$	Divergence factor
$\xi$	Path difference phase variable
$d_1$	Distance from transmitter
$d_2$	Distance from receiver
$r$	Radius of curvature of earth
$a$	Earth radius
$a_e$	Effective earth radius
$h$	Height above earth surface ( Chapter 3)
$d$	Total path length
$h_c$	Clearance height of obstruction
$V(X)$	Attenuation factor
$U(Z)$	Height gain function
$F_d$	Path gain factor due to diffraction
$H_1$	Radius of first Fresnel zone
$S/N$	Signal to noise ratio

<u>Symbol</u>	<u>Description</u>
$h$	Plank's constant ( Chapter 4)
$K$	Boltzman constant
$R$	Resistance (Chapter 4)
$B_n$	Band width
$NF$	Noise figure
$N_{in}$	Noise input
$N_{out}$	Noise output
$S_{in}$	Signal input
$S_{out}$	Signal output
$G$	Gain of the system
$dB$	Decibel
$T_r$	Effective input noise temperature
$\Delta N$	Noise difference between input and output
$N_0$	Receiver noise
$C_{min}$	Received carrier level
$P_T$	Transmitter output power
$P_R$	Receiver output power
$G_T$	Directivity gain of transmitting antenna
$G_R$	Directivity gain of receiving antenna
$G_s$	System gain
$A_{eff}$	Effective area of receiving antenna
$P_{Di}$	Radiate power per unit area of antenna

<u>Symbols</u>	<u>Description</u>
EIRP	Effective isotropic radiate power
$L_{dB}$	Line loss
$L_{Feed}$	Feeder loss
$L_B$	Branching network loss
$G_{dB}$	Antenna gain
FM	Fade margin

## Abstract

Interference in microwave space-wave propagation occurs when two waves from the same source meet at a point after traveling through separate paths. In case of microwave propagation, the waves reach the receiving point not directly (line-of-sight path) but also after being reflected from the ground. If the frequency and height of antenna is such that the difference between the direct and the ground reflected wave exactly equals one wave length, the two waves completely or partially cancel depending on the constants of the earth, but if the path difference equals half wavelengths, reinforcement of received waves take place. A succession of such points lie one above the other giving an interference pattern having alternate cancellation and reinforcements. Such patterns can be plotted from the actual field strength measurements or by actual calculation. The evaluation of a proposed communication link must be carried out with due attention given to these interference effects. The goal would be to ensure that sufficient signal-to-noise margin is available so that under adverse propagation conditions outages will occur for only small intervals of time.

Interference effects are analyzed for microwaves (above 1GHz) and a computer model is developed to obtain radiation patterns (lobes and nulls) due to interference. Appropriate formulas for the interference effects due to antennas located over a flat earth and over a spherical earth, for field in the diffraction zone and for calculating midpath obstacle (hills and buildings) diffraction loss are used to develop the model. Effects of earth's curvature, earth's imperfections and roughness, shadowing effects of hills and buildings on the field strength in the interference zone are incorporated in the model.

The model is used to calculate the signal-to-noise margin, path gain factor, maximum link distance corresponding to a particular earth's surface, frequency and height of the antenna, the incident power per unit area at the receiving terminal, the field for a microwave link. Specific results for a number of UHF and SHF links have been obtained and compared with datas taken from Bangladesh T. & T. Board. The agreement between the two results is found to be satisfactory.



# CHAPTER 1

## INTRODUCTION

### 1.1 PROPAGATION OF ELECTROMAGNETIC WAVES AND INTERFERENCE EFFECT

There are many possible propagation paths to reach the radiated energy from the transmitting antenna to the receiving antenna. Some of them are shown in fig 1.1.

Waves scattered by the troposphere [5,11] are called tropospheric waves. Some of these arrive at the receiver after reflection or scattering in the ionosphere are named sky wave. Energy propagated over other paths near the earth surface is termed ground wave. It is divided into two parts such as the space wave and the surface wave. The space wave is again divided into two parts. The signal that travels through the direct path from transmitter to receiver is called direct wave and the signal arriving at the receiver after being reflected from the surface of earth is termed as ground reflected wave. The surface wave is called the 'Norton surface wave' and is usually guided along the earth's surface.

In communication phenomena interference occur whenever there are two or more paths through which the waves can propagate along to reach the receiving antenna. Fading [1,3,8] takes place

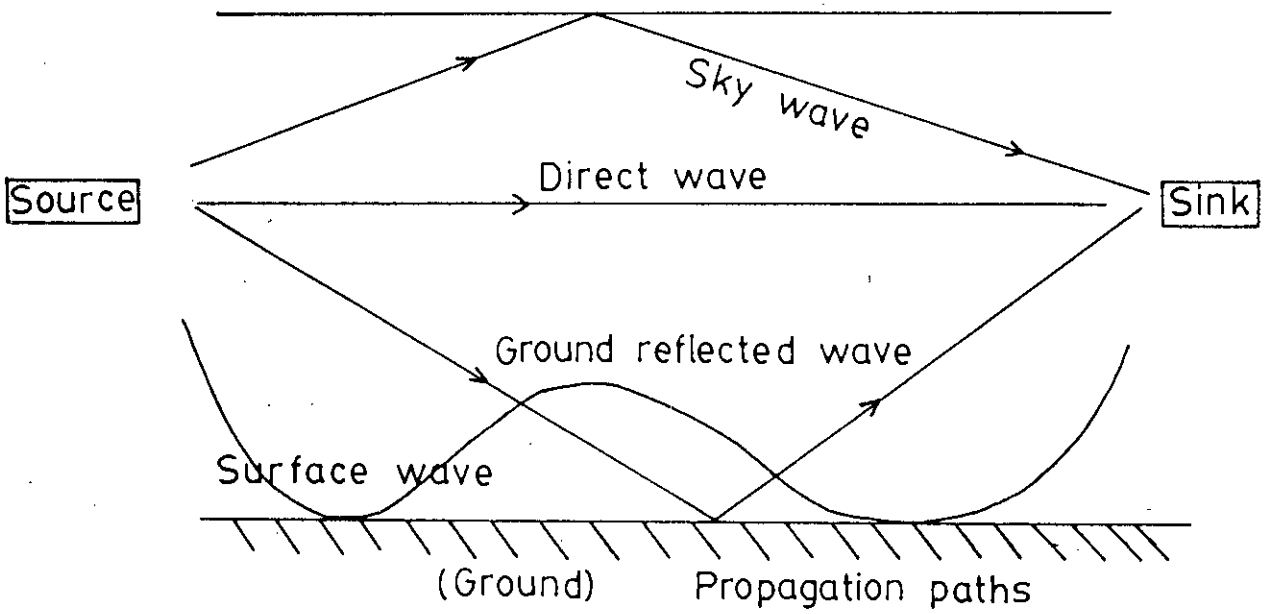


Fig.1.1 Illustration of propagation paths

if the propagation path is not stable and as a result large variation in the received signal power takes place over time intervals. The instability in the propagation path is due to the variation of index of refraction of atmosphere which is the function of temperature and humidity. Variations in the index of refraction [5,12] cause the phase angle of the signal arriving at the receiving site to vary in a random way. Thus signals arriving along different paths combine more or less with random phases. As a result of these phase differences often these signals tend to cancel one another. This may cause fading. Generally, some diversity techniques are used to overcome the above effects.

The propagation of the electromagnetic energy between the transmitting and receiving antennas takes place under free-space condition . Free space propagation essentially occurs for some communication links under ideal conditions. However, for most communication links the signal propagation is modified by the presence of the earth, the atmosphere, the ionosphere and atmospheric hydrometeors such as rain fall, snow, hail etc. The influence of the natural environment on propagation of radio wave is highly dependent on the frequency and the proximity of the antennas to the ground.

## 1.2 PROPAGATION DUE TO FREQUENCY RANGE

The propagation mode of a radio wave is closely dependent upon its frequency. Here some broad frequency intervals that influence the radio-wave propagation are described.

In case of extremely low frequencies the wavelength is greater than 100 km. The antennas used are very large and are of necessity close to the ground. Transmission in this range is primarily due to surface wave because of relatively low ground attenuation. The sky wave is reflected [1,6] from the ionosphere and a form of earth-ionosphere waveguide exists that may be thought of as providing a guiding path for the waves as they propagate around the earth.

As the frequency is increased above 30 kHz the propagation is strongly influenced by the presence of the ground. The sky wave attenuation is less in the lower range of this band of frequencies but increases in the higher range such as 30 kHz or above. In general, the day time sky wave absorption is relatively high in the ionosphere and long distance communication is uncertain due to varying conditions of ionosphere. But long-range night communication via sky wave is reliable. At the higher range of medium frequencies (around 2-3 MHz) the sky waves are highly attenuated and the only reliable communication during day is by

surface wave propagation.

Frequency range from few MHz up to 30 MHz to 40 MHz include the international shortwave broadcasting and radio wave reflected from the ionosphere to provide communication over long skip distances. Over the propagation path, free-space propagation conditions are approached, but the variability of the electron concentration with of day, yearly variations etc., produces a considerable amount of fading as well as periods of time when only certain frequencies are usable.

A sky wave above 50 MHz [1,6] does not return to earth and pass out into space. The surface wave are rapidly attenuated due to heavy ground losses. Hence transmission in this range is effected by space wave. The antennas are relatively small and the main propagation effects are those associated with interference between the signals which propagate along the direct line-of-sight path and those reflected from ground. At SHF range and above, attenuation and scattering occur due to rain and atmospheric gases. The diffraction [1] of the waves due to hill, buildings, trees etc. are also much more pronounced in this range. Our proposed thesis work is based on this band of frequencies.

In the region of millimeter wavelength atmospheric attenuation as well as attenuation due to rain becomes a serious

factor in the distance between transmitting and receiving antennas. This attenuation is exponential in character and it can severely limit the propagation distance.

### 1.3 FREQUENCY BAND DESIGNATION

The different bands of frequencies and standard band designation [1,3,11] are shown in the table-1. The microwave and millimeter frequency bands are broken down into several bands designated by letters. These are discussed in appendix A.

Table-1

Desingnation	Frequency Band	Typical service
Very Low Frequencies (VLF)	3-30 kHz	Navigation, sonar
Low Frequencies (LF)	30-300 kHz	Radio beacons
Medium Frequencies (MF)	300-3000 kHz	AM broadcasting, maritime radio
High Frequencies (HF)	3-30 MHz	Telephone, telegraph, facsimile
Very High Frequencies (VHF)	30-300 MHz	Television, FM broadcast, police
Ultra High Frequencies(UHF)	300-3000 MHz	Television, satellite communication
Super High Frequencies (SHF)	3-30 GHz	Airborne radar, MW links, satellite
Extra High Frequencies (EHF)	30-300 GHz	Radar
Microwave Frequencies	MWF	Generally Above 1 GHz

## CHAPTER 2

# RADIOWAVE INTERFERENCE PHENOMENA OVER FLAT EARTH

### 2.1 INTRODUCTION

When a plane radio wave strikes the surface of earth it is reflected with an angle of reflection equal to the angle of incidence. Reflected wave changes in magnitude as well as in phase. Vector ratio of reflected to incident wave is called reflection co-efficient. The reflection co-efficient depends in a complex way upon frequency, dielectric constant, conductivity of earth, plane of polarization and angle of incidence of the wave on the earth.

### 2.2 GENERAL FEATURES OF INTERFERENCE PHENOMENA WITH ANTENNAS LOCATED OVER A FLAT-EARTH

The general features of interference phenomena associated with antennas placed over earth can be determined by studying the effects associated with antennas located over a flat-earth. The radiation field strength patterns [1,5,13] of transmitting antenna and receiving antenna are  $f_1$  and  $f_2$  respectively and  $h_1$  and  $h_2$  are the respective heights for the two antennas shown in the figure 2.1 [1,5,13].

With reference the figure 2.1 the field that reaches the receiving antenna directly produces voltage which is proportional

to

$$f_1(\theta_1)f_2(\theta'_1)e^{(-jk_0R_1)}/(4\pi R_1)$$

and voltage produced by the indirect or reflected wave is proportional to

$$f_1(\theta_2)f_2(\theta'_2)\rho e^{(j\phi)}e^{-jk_0R_2}/(4\pi R_2)$$

where  $\rho e^{j\phi}$  is the reflection coefficient at the ground and  $k_0$  is the propagation constant.

In the usual situation  $h_1$  and  $h_2$  are very small compared with the span distance  $d$ ; hence the angles  $\theta_1$ ,  $\theta_2$ ,  $\theta'_1$  and  $\theta'_2$  are very small and the antenna patterns can be assumed constant over the range of angle involved. Therefore total received voltage will be proportional to

$$f_1(\theta_1)f_2(\theta'_1)e^{(-jk_0R_1)}/(4\pi R_1)+f_1(\theta_2)f_2(\theta'_2)e^{(-jk_0R_2)}\rho e^{(j\phi)}/4\pi R_2 \dots\dots\dots(2.01)$$

As the span distance  $d$  is very large we can simplified the above equation taking  $R_1=R_2$  for the denominator as

$$f_1(\theta_1)f_2(\theta'_1)\frac{e^{-jk_0R_1}}{4\pi R_1}\left|1+\rho e^{j\phi}\frac{f_1(\theta_2)f_2(\theta'_2)e^{-jk_0(R_2-R_1)}}{f_1(\theta_1)f_2(\theta'_1)}\right|$$

$$= f_1(\theta_1)f_2(\theta'_1)e^{-jk_0R_1}/4\pi R_1 \cdot F$$

where  $F=|1+\rho e^{j\phi}\frac{f_1(\theta_2)f_2(\theta'_2)e^{-jk_0(R_2-R_1)}}{f_1(\theta_1)f_2(\theta'_1)}|\dots\dots(2.02)$  is called the path-gain factor [1,5,6,11], shows how the field at the receiving antenna differs from the value it would have under free-space propagation condition.



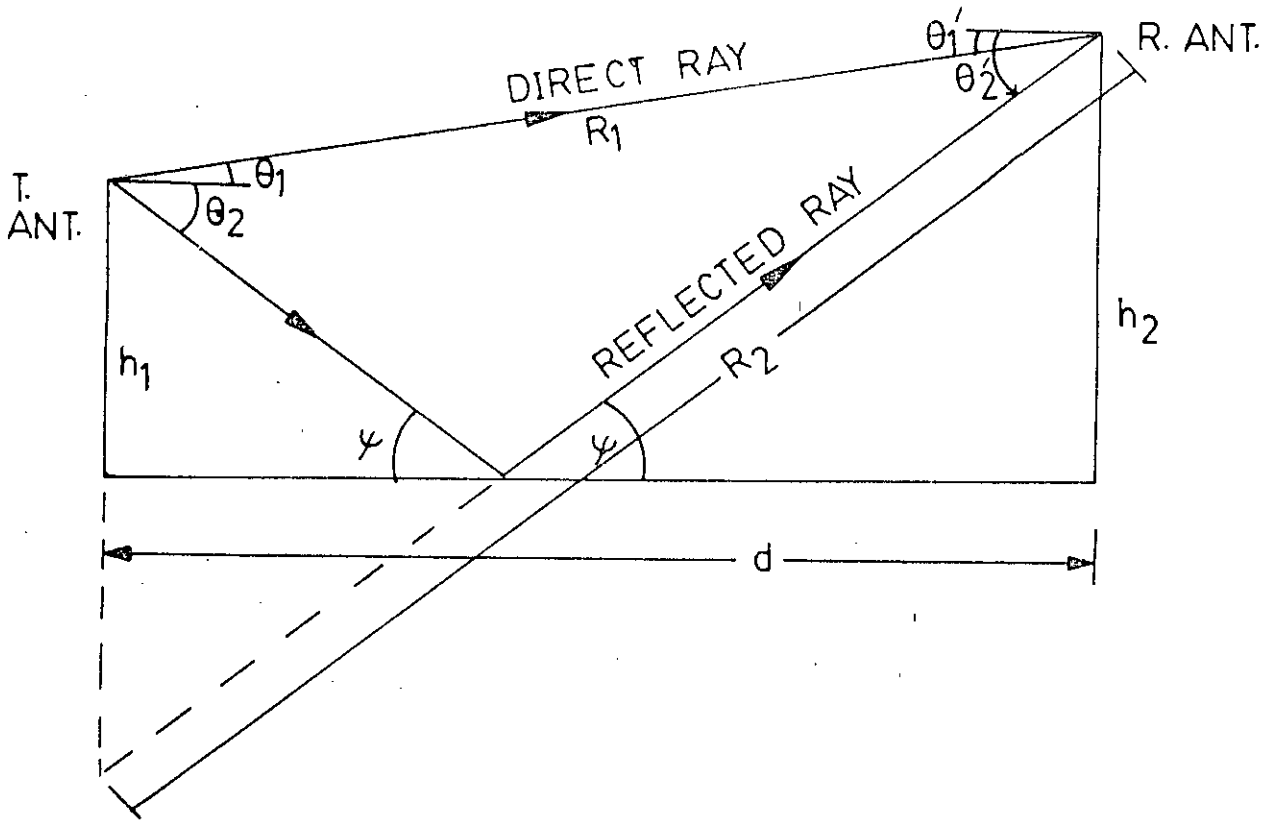


Fig.2.1 Illustration of direct and reflected rays.

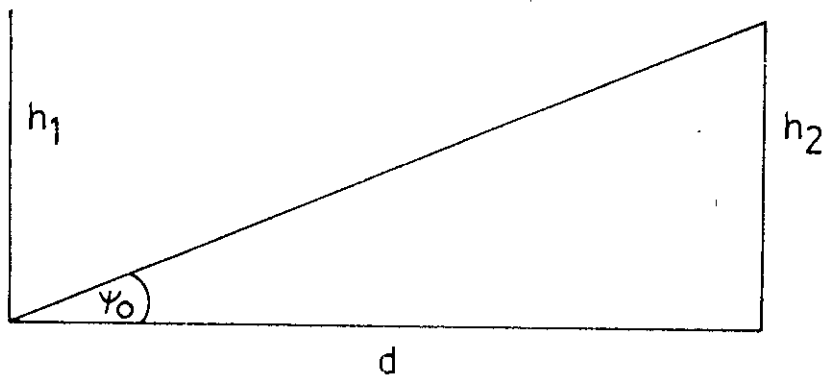


Fig.2.2 Illustration of elevation angle.

If  $f_1(\theta_1) \cong f_1(\theta_2)$  and  $f_2(\theta'_1) \cong f_2(\theta'_2)$  we can express F as

$$F = |1 + e^{j\phi - jk_0(R_2 - R_1)}| \dots\dots\dots(2.03)$$

With the reference to the figure 2.01 we have,

$$R_1 = \{d^2 + (h_2 - h_1)^2\}^{0.5}$$

$$= d + (h_2 - h_1)^2 / (2d)$$

$$R_2 = \{d^2 + (h_1 + h_2)^2\}^{0.5}$$

$$= d + (h_2 + h_1)^2 / (2d)$$

and  $R_2 - R_1 = 2h_1h_2/d \dots\dots\dots(2.04)$

If we consider  $\rho e^{j\phi} = -1$  which is good for many of the practical cases then the above calculated value we have

$$F = |1 - e^{-j2k_0h_1h_2/d}| \dots\dots\dots(2.05a)$$

$$= |1 - \cos(2k_0h_1h_2/d) + j\sin(2k_0h_1h_2/d)|$$

$$= 2|\sin(k_0h_1h_2/d)| \dots\dots\dots(2.05b)$$

It is clear from the above equation that interference effects can lead to a doubling of the field strength relative to the value under free space condition. Hence the path-gain factor can be expressed in term of elevation angle referring to the figure 2.02 as

$$F = 2\sin(k_0h_1 \tan \psi_0) \dots\dots\dots(2.06)$$

Therefore F is maximum when

$$\tan \psi_0 = (\pi/2 + n\pi) / k_0h_1$$

$$= (1/4 + n/2)\lambda_0 / h_1 \dots\dots\dots(2.07a)$$

where  $n=0, 1, 2, \dots$

and F is minimum when

$$\begin{aligned} \tan \psi_0 &= \pi / (k_0 h_1) \\ \Rightarrow \tan \psi_0 &= n \lambda / (2h_1) \dots \dots \dots (2.07b) \end{aligned}$$

The phase change between the direct and the reflected component due to the path difference  $(R_2 - R_1) = \delta$  radians and the total phase shift between the direct component  $E_d$  and the reflected component  $E_r$  ( $E_r$  lagging  $E_d$ ) is  $180^\circ + \delta$ , where  $\delta$  is expressed in degree (shown in Fig 2.3). Since the path difference  $\Delta R$  is negligible the two component are almost equal in magnitude. Therefore from the diagram 2.3

$$\begin{aligned} E^2 &= E_r^2 + E_d^2 + 2E_r E_d \cos(\pi - \delta) \\ &= 2E_d^2 (1 - \cos \delta) \end{aligned}$$

$$\text{Hence } E = 2E_d \sin(\delta/2) \dots \dots \dots (2.08a)$$

If  $\delta$  is very small,  $\sin(\delta/2) \cong \delta/2$ , the field strength is then

$$\begin{aligned} E &= E_d \delta \\ &= 4\lambda E_d h_1 h_2 / (d \lambda_0) \dots \dots \dots (2.08b) \end{aligned}$$

The above discussion is based on  $\rho = 1$  and  $\phi = 180^\circ$ .

### 2.3 REFLECTION CO-EFFICIENT FOR PROPAGATION

The reflection co-efficient  $\rho e^{j\phi}$  is given by the Fresnel expressions for the reflection co-efficient for a plane wave polarized with the electric field in the plane of incidence (vertical polarization) and for a wave polarized with the

electric field perpendicular to the plane of incidence (horizontal polarization). The Fresnel reflection co-efficients depend on the ground conductivity, permittivity, frequency and angle of incidence.

The reflection co-efficient for vertical and horizontal polarization [1,2,5] are calculated using the following equations.

$$R_v = \rho e^{j\phi} = \frac{(k-j\chi)\sin(\psi) - [(k-j\chi) - \cos^2(\psi)]^{0.5}}{(k-j\chi)\sin(\psi) + [(k-j\chi) - \cos^2(\psi)]^{0.5}} \dots\dots\dots(2.09)$$

$$R_h = \rho e^{j\phi} = \frac{\sin(\psi) - [(k-j\chi) - \cos^2(\psi)]^{0.5}}{\sin(\psi) + [(k-j\chi) - \cos^2(\psi)]^{0.5}} \dots\dots\dots(2.10)$$

where  $\chi = \delta/w\epsilon_0$

$\delta$  = Ground conductivity,

$\epsilon_0$  = Permittivity

$\psi$  = The grazing angle of incidence

Some typical values of the above parameters are given below

Dielectric constant(k) = 15 (approx.)

(It may smaller for poor conductivity of soil and will increase upto about 30 for soil with high conductivity)

Ground Conductivity( $\delta$ ) = from  $10^{-3}$  to  $3 \times 10^{-2}$  S/m

When the incident wave is normal to the reflecting surface ( $\psi = 90^0$ ) there is no difference between the horizontal and vertical polarization ( Fig. 2.4 ). In both cases the electric

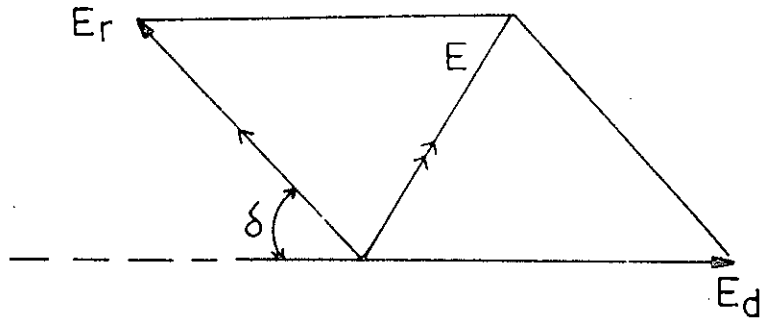
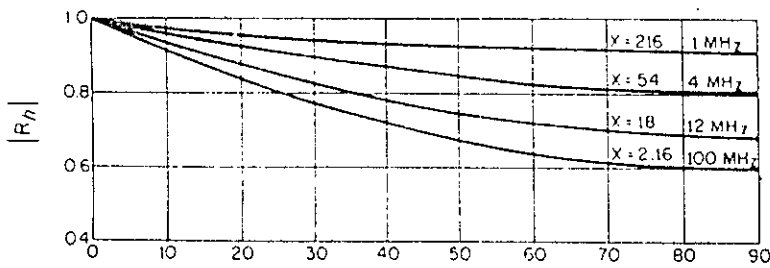
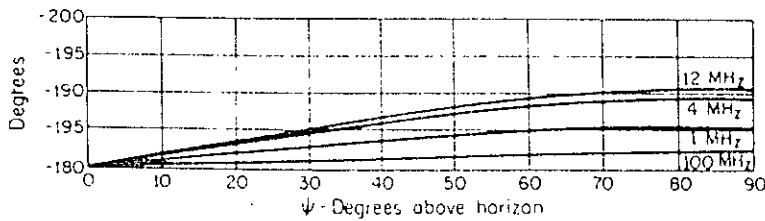


Fig.2.3-Phasor diagram of resulted field strength and phase.



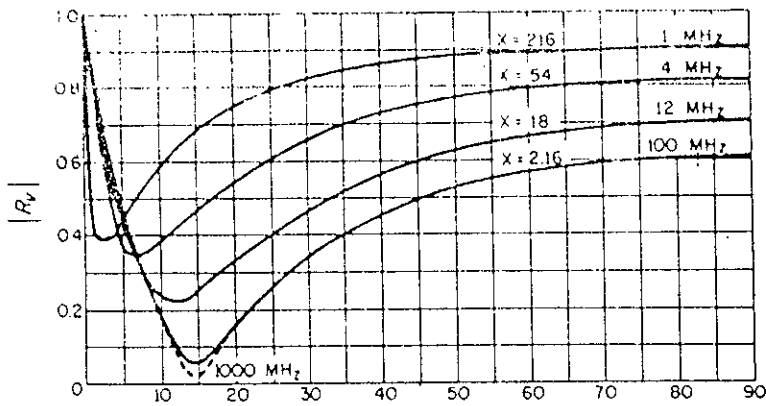
(a)



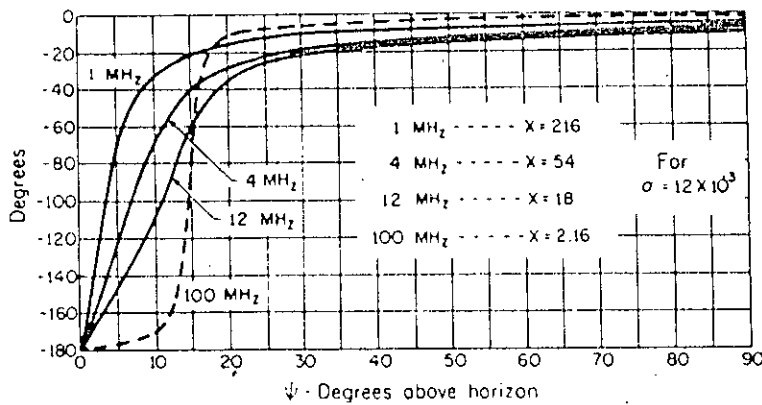
(b)

Fig.2.4 Reflection co-efficient for horizontal polarization with  $\sigma = 12 \times 10^{-3}$  and  $\epsilon = 15$ .  
 (a) Magnitude of reflection co-efficient  
 (b) phase of reflection co-efficient

( These figures are taken from reference 5 )



(a)



(b)

Fig.2.5 Reflection co-efficient for vertical polarization with  $\sigma = 12 \times 10^{-3}$  and  $\epsilon = 15$ .

(a) magnitude of reflection co-efficient

(b) Phase of reflection co-efficient

( These figures are taken from reference 5 )

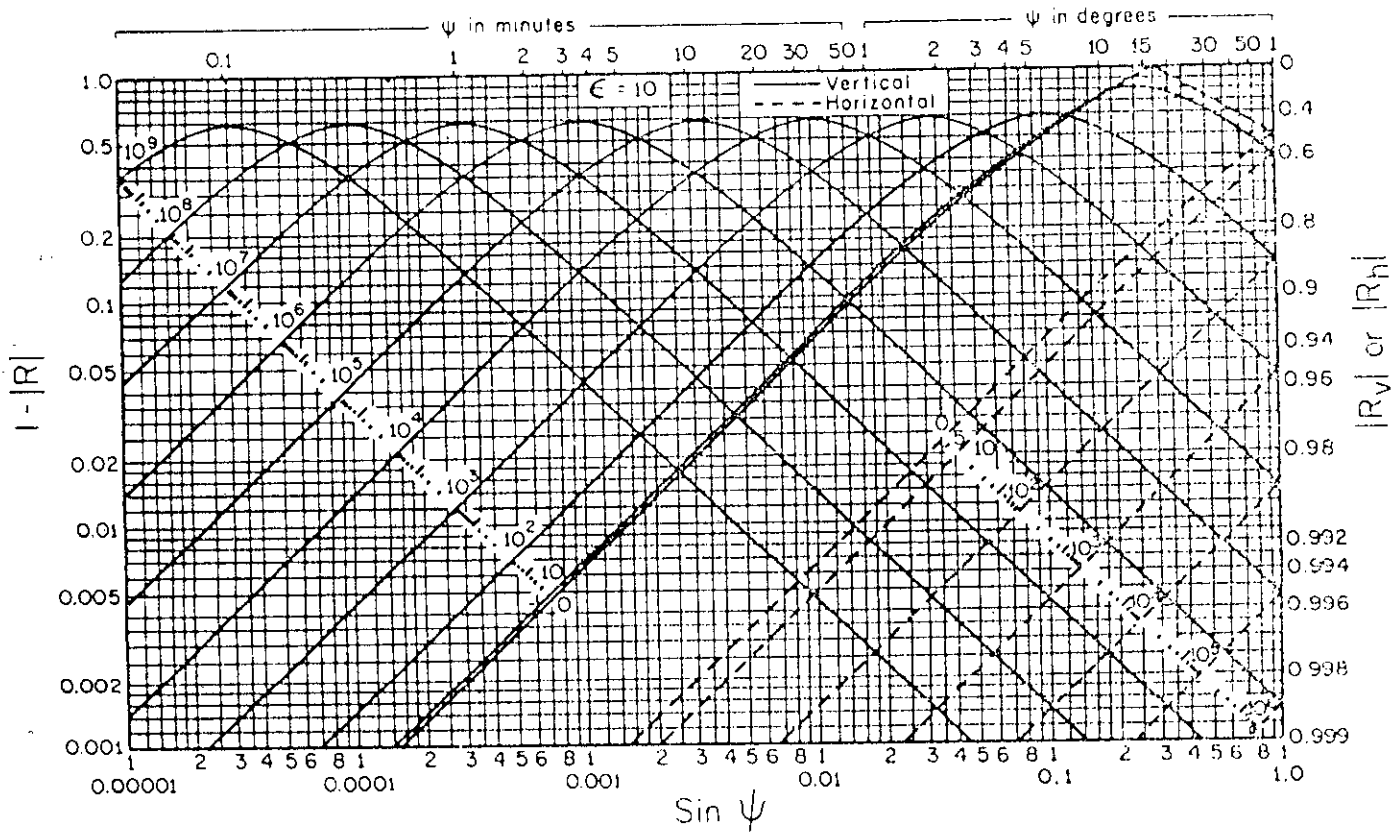


Fig.2.6 Magnitude of the reflection co-efficient for  $\epsilon_r=15$ .  
 The number of each curve gives the value  $X=18 \times \delta / f_{\text{MHz}}$ .  
 [Vertical polarization is shown by solid lines]

( This figure has been taken from reference 5 )

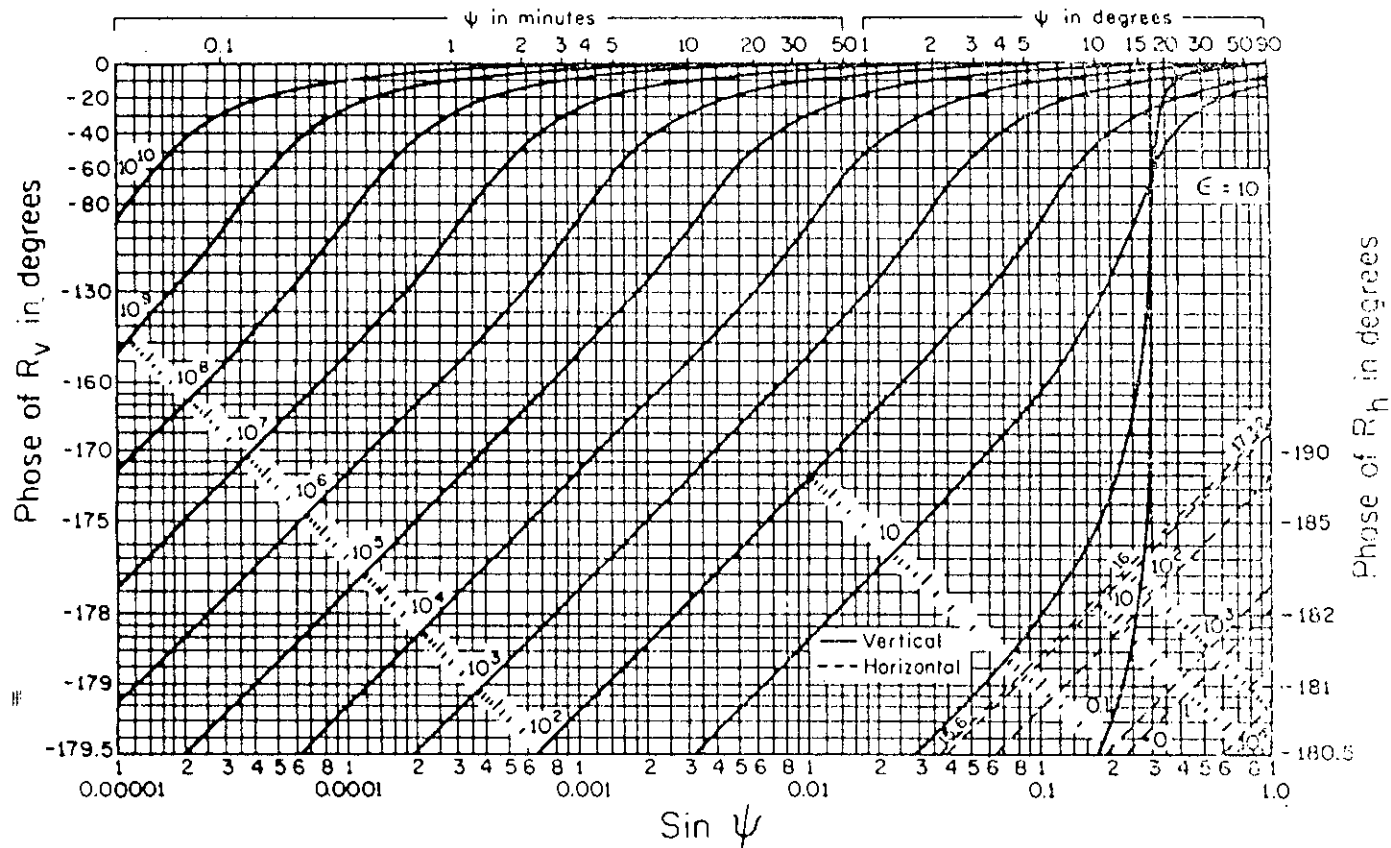


Fig.2.7 Phase of the reflection co-efficient for  $\epsilon = 10$ .  
 [Vertical polarization is shown by solid lines and  
 horizontal polarization is shown by dotted lines]

( This figure has been taken from reference 5 )



vector will be parallel to the reflecting surface and the reflecting co-efficient  $R_v$  and  $R_h$  should have the same value. But there is  $180^\circ$  phase difference. The magnitudes and phases of the reflection co-efficients are shown on a logarithmic scale for a relative dielectric constant  $\epsilon = 10$  in fig.2.5 and fig.2.6 respectively. These curves are labelled directly in the value of  $X$ .

From fig.2.4 and fig.2.5 it is clear that there is particular significance of Brewster angle effect for vertical polarization, which causes  $\rho$  a minimum for values of  $\psi$  below  $15^\circ$ . The phase angle also goes a rapid change from  $0^\circ$  to  $180^\circ$ . This effect makes  $e^{j\phi}$  nearly equal to  $-1$  for both vertical and horizontal polarization when the grazing angle  $\psi$  tends to zero. When the frequency increases  $X$  decreases (As  $X = \sigma/w\epsilon_0$ ). As a result frequencies above 50 MHz the ground behaves very nearly like a dielectric medium.

#### 2.4 PATTERNS OF COVERAGE DIAGRAM

Coverage diagram is the plot of relative field strength as a function of direction in space from the transmitting antenna. It is analogous to the field strength radiation pattern of an antenna. The fixed parameters are the height of the transmitting antenna ( $h_1$ ) and the wave length ( $\lambda_0$ ) or frequency ( $f$ ). The

height of receiving antenna ( $h_2$ ) and the distance  $d$  to the location of the receiving antenna are variable parameters. Each pair of  $h_2$ - $d$  determines a point in space.

In general the coverage diagram is the plot of curves for  $F/r$  is constant in the  $h_2$ - $d$  plane (Where  $r$  is the direct line-of-sight distance). In most situation the direct line-of-sight distance is equal to horizontal distance ( $d$ ). Various curves of  $F/r$  are usually chosen to represent the same signal level which would be obtained a fractional or multiple of convenient free-space reference range  $r_f$ .

$$\begin{aligned} \text{i.e. } F/r &= m/r_f \\ \text{or, } F &= mr/r_f \\ &\cong md/r_f \dots\dots\dots(2.11) \end{aligned}$$

where  $m = 1, \sqrt{2}, 2, \dots\dots$  or  $1, 1/\sqrt{2}, 1/2, \dots\dots$  etc.

The difference of successive curve is then 3.0 dB.

#### 2.4.1 STUDY OF DIFFERENT CASES

Case 01 : Reflection- coefficient equal to -1.

The flat earth formulla is therefore,

$$\begin{aligned} F &= 2|\sin(k_0 h_1 h_2 / d)| \\ &= 2|\sin(k_0 h_1 \tan \psi_0)| \end{aligned}$$

$$\text{i.e. } 2|\sin(k_0 h_1 \tan \psi_0)| = md/r_f \dots\dots\dots(2.12)$$

Here  $d$  can be treated as radial co-ordinate and  $\psi_0$  as the angle

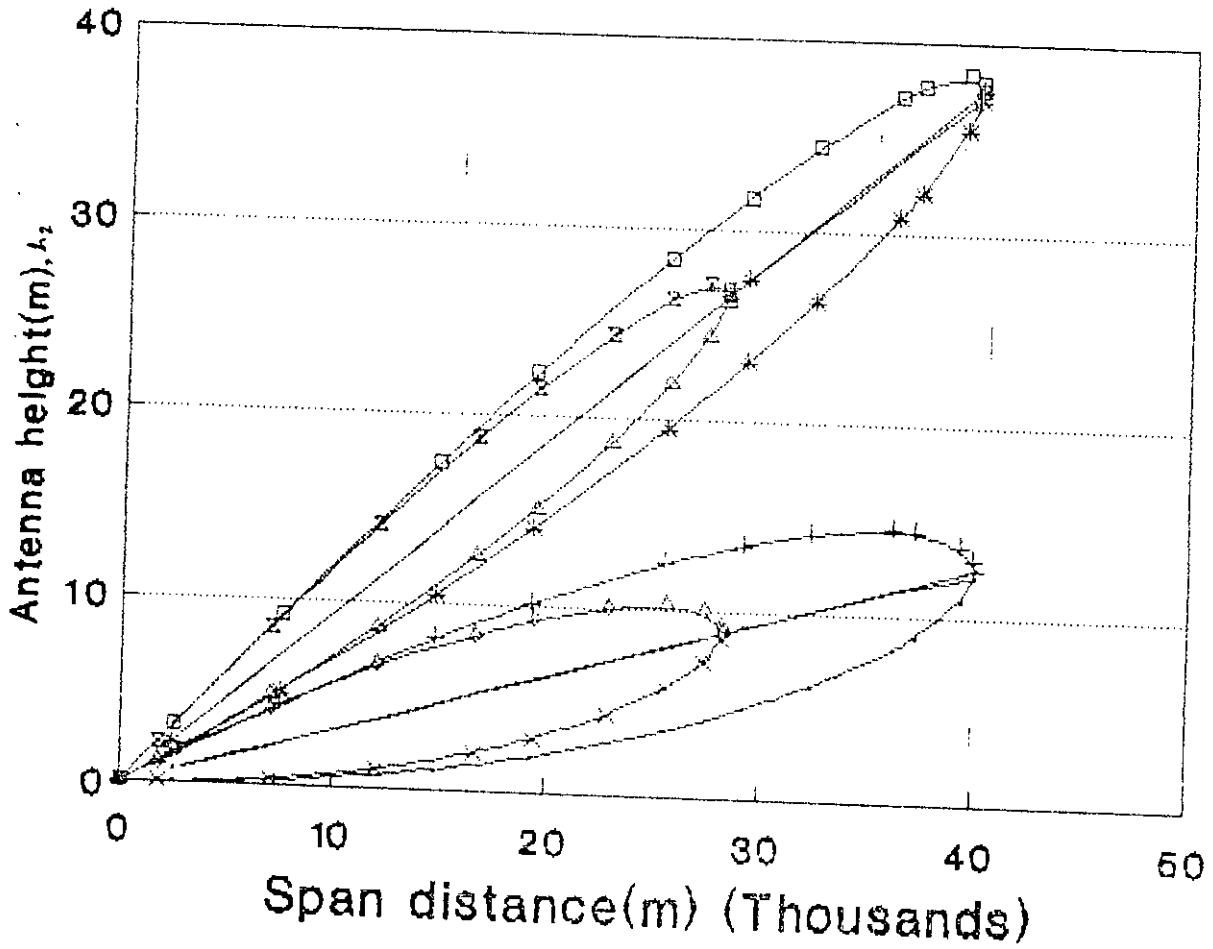


Fig.2.8 - Coverage diagram for  $h_1=800\lambda_0$ ,  $r_f=20\text{km}$ .  
 ( It is the plot of curves for  $F/r$  is constant in the  $h_2$ -d plane)

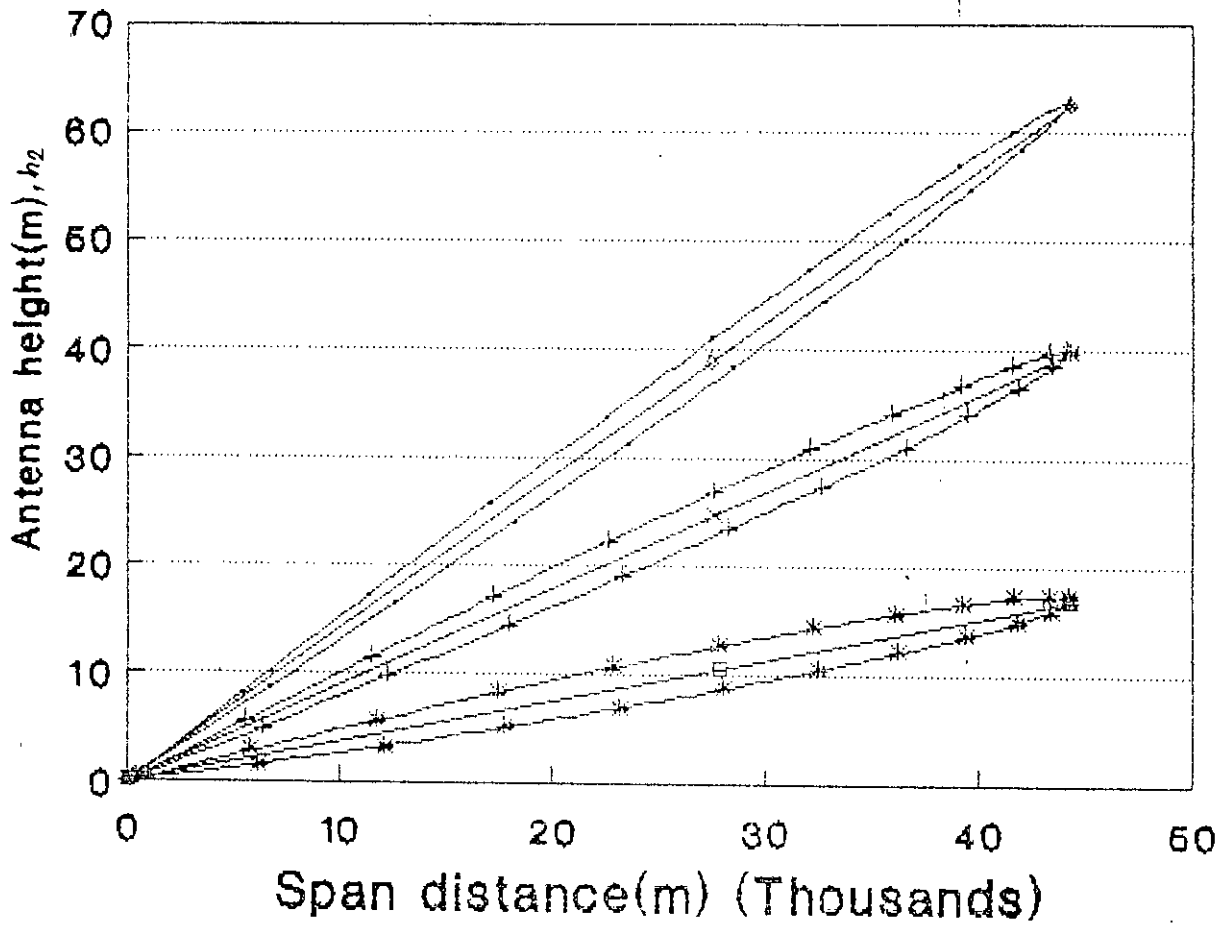


Fig.2.9 Coverage diagram for  $h_1=1625\lambda_0$ ,  $r_f=22.15\text{km}$ .  
 ( It is the plot of curves for  $F/r$  is constant in the  $h_2$ - $d$  plane)

co-ordinate in a polar-co-ordinate reference frame. However the vertical scale representing by  $h_2$  is usually expanded relative to that for  $d$ . Hence  $\theta_0$  appears much larger than its actual value.

when  $h_1 \gg \lambda_0$  and  $n$  is small we have  $\tan(\psi) = \psi$ . From equation 2.06 and 2.07 a very fine lobe structure is obtained. The maximum interference range is in this case is  $2r_f$  which comes from the horizontal span  $d = 2r_f \cos(\psi_0)$ . Some curves are drawn shown in the Fig.2.8 and fig.2.9. Smaller lobes are drawn in the figure 2.8 represent a constant signal level 3 dB greater than that of the larger lobe. Several lobes are shown in the figure 2.9.

Case 02:- Reflection co-efficient not equal to -1.

Using Fresnel expression for reflection co-efficient we can develop a computer sub-program which supply essential datas to the main program. The procedure is same as in the case of 01.

## 2.5 EFFECT OF ROUGHNESS IN PROPAGATION

When the point of reflection occurs over a rough surface the field is scattered in a more diffuse manner and the specular reflected component and hence reflection co-efficient is reduced in value. Considering the effective wave length of the incident wave we can measure the surface irregularities that constitute a rough surface [5,11]. We can calculate the propagation factor

equal to  $e^{jk_0z} \sin(\psi) - jk \ x \ \cos(\psi)$  for incident wave, where  $z$  and  $x$  are the co-ordinate in the perpendicular to the surface and along the surface respectively. Hence in vertical direction the wave length  $\lambda_v$  is given by

$$\begin{aligned} \lambda_v &= (2\pi)/(k_0 \sin\psi) \\ &= \lambda_0/\sin\psi \quad \dots\dots\dots(2.12) \end{aligned}$$

When the grazing angle  $\psi$  is small  $\lambda_v$  is large compare to  $\lambda_0$ . At larger wavelengths most surfaces appear to be smoth, but at microwave frequencies most surfaces would be rough and the reflection co-efficient would be smaller than that given by the Fresnel formulas.

## 2.6 VARIATION OF SPACE WAVE FIELD STRENGTH WITH DISTANCE

From fig.2.1 it is clear that the difference in path length between the direct and reflected rays decreases as the distance increases. It has been shown for small elevations the reflected wave suffers a phase change of very nearly  $180^\circ$  at the point of reflection. Therefore, where the path difference between the rays in an exact number of wave lengths the two rays will be  $180^\circ$  out of phase and so will substract. The two rays will not cancel each other completely since imperfect reflection at the ground makes the reflected wave of a smaller magnitude than the

direct ray. Thus the resultant amplitude of field strength is less than that of direct wave alone. When the path difference is exactly a half wave length or an odd number of half wave lengths the direct and reflected rays are in phase and the two will add giving a field strength greater than that of direct ray alone. If we simplify the equation no. 2.05b considering  $\psi_0$  as low then the received signal varies as the inverse square of the distance as shown in fig.2.10 [1,5,6,11].

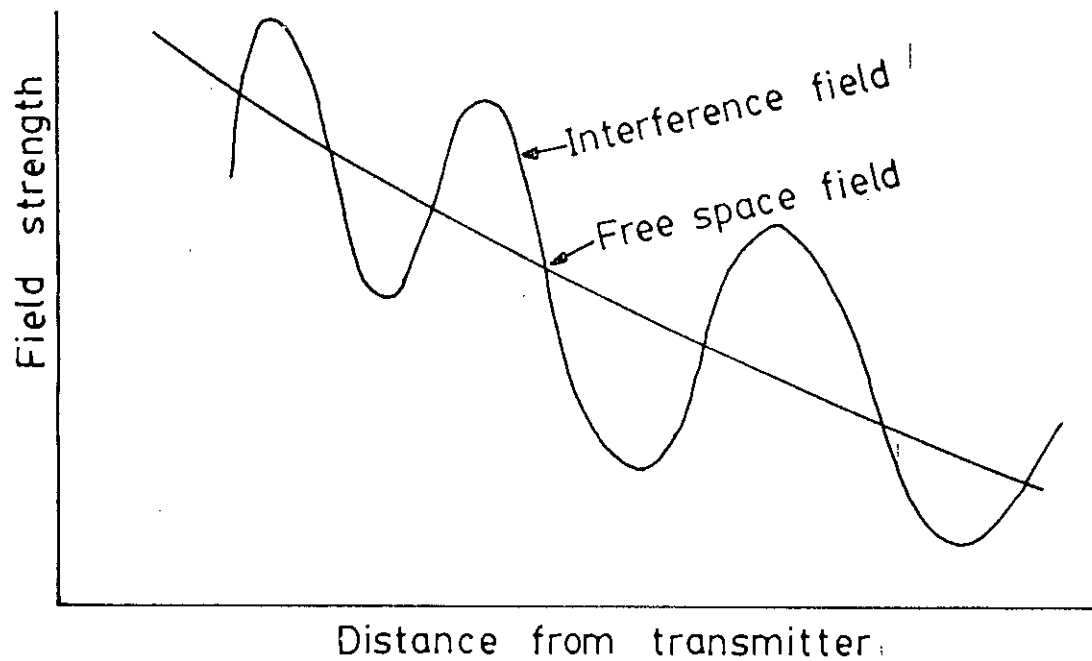


Fig.2.10 A typical plot of field strength against distance from transmitter.



# CHAPTER 3

## RADIOWAVE PROPAGATION PHENOMENA OVER SPHERICAL EARTH

### 3.1 EFFECT OF CURVATURE OF EARTH IN PROPAGATION AND ATMOSPHERIC EFFECTS

A radio wave travelling horizontally in the earth's atmosphere follows a path which has a slight downward curvature due to refraction of the wave in the atmosphere [1,3,12]. This curvature of the path tends to overcome partially the loss of signal due to curvature of the earth and permits the direct ray to reach points slightly beyond the horizon as determined by the straight line path.

The refraction of a radio wave in the atmosphere occurs because the dielectric constant and hence the refractive index of the atmosphere, varies with height above the earth. The dielectric constant of dry air is slightly greater than the value of unity that applies for a vacuum and the presence of water vapor increases the dielectric constant still further. For this reason the dielectric constant of the atmosphere is greater than unity near the earth's surface, but decreases to unity at great heights where the air density approaches zero. The refractive index  $n$  is related with the refractivity  $N$  by  $N=(n-1)10^6$  (NU). The refractivity can be calculated through the relation.

$$N(n-1)10^6 = \frac{77.6}{T} P + 4810 \frac{e}{T^2} \dots\dots\dots(3.01)$$

where P = total pressure (m bar)

e = partial pressure of water vapor (m bar)

T = Absolute temperature (degree kelvin)

Under normal conditions of the atmosphere both temperature and pressure fall with the height above earth's surface in the troposphere region [5,6,12]. The gradient of index of refraction is associated with the temperature and pressure gradients and hence varies with height. Thus the communication through space wave propagation is obtained by beyond the line-of-sight as shown in fig.3.1.

The phenomena of ray curvature may be readily understood by dividing the atmosphere into layers, with discrete values for the index of refraction in each layer, as shown in Fig.3.2 [1,5,6]. For this staircase approximation to the continuous variation in the index of refraction Snell's law gives.

$$n_1 \sin \theta_1 = n_2 \sin \theta_2 = \dots\dots\dots = n_n \sin \theta_n \dots\dots\dots(3.02)$$

where  $n_1 > n_2 > n_3 > \dots\dots\dots > n_n$

and  $\theta_n > \theta_{n-1} > \theta_{n-2} > \dots\dots\dots > \theta_2 > \theta_1$

The empirical expression as:

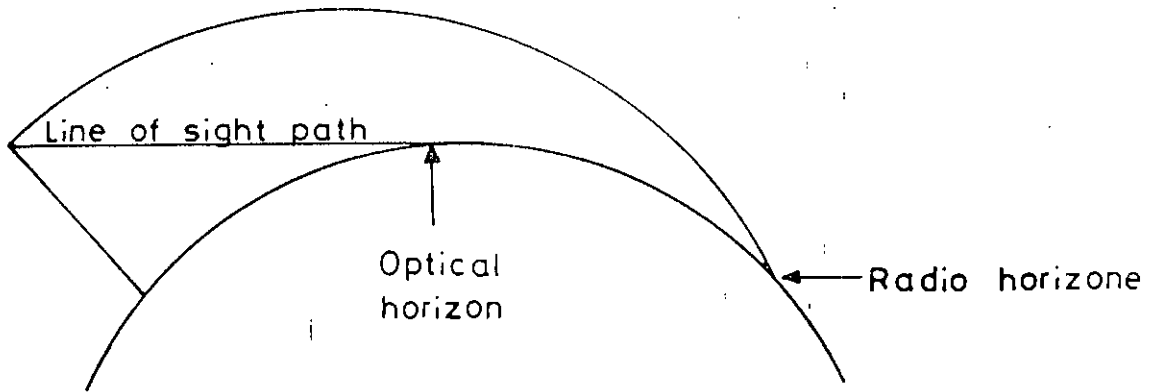


Fig.3.1 Illustration of radio horizon and optical horizon

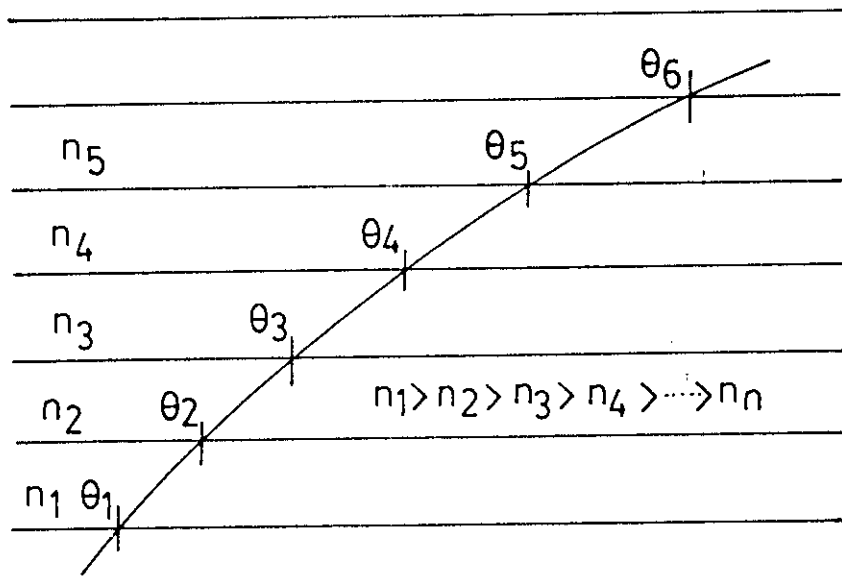


Fig.3.2 Illustration of ray curvature

$$N(h) = N_s e^{C_e h} \quad \text{NU}$$

$$C_e = \ln \frac{N_s}{N(1\text{km})} = \ln \frac{N_s}{N_s + \Delta N}$$

where  $N_s$  is the refractivity at the earth surface and  $h$  is the height above ground (km).  $\Delta N$  is the difference between the radio refractivity at the height of 1 km that at earth surface.

Under abnormal conditions the changes in temperature and moisture content in the atmosphere are such that the refractive index increases with height as a result in the bending of waves away from the earth. A typical abnormal condition occurs when there is warm air over water resulting in a high density of water vapor over the surface. Under this condition the atmosphere forms a wave guide that guides the waves over the surface.

### 3.2 MATHEMATICAL ANALYSIS FOR EFFECTIVE EARTH RADIUS

The effect of refraction in troposphere may be consider in terms of straight line path propagation by simply increasing the effective radius of the earth [5,6,12]. Consider a wave to be travelling almost horizontally in the troposphere. Its path bends into an arc due to variation of refractive index with height. Let  $r$  is the radius of curvature of the path at a height  $h$  above earth's surface and  $v$  be the velocity at that height.

From Figure 3.3

$$rd\theta = vdt$$

$$\text{and } (r+dh)d\theta = (v+dv)dt$$

Hence  $dh d\theta = dv dt$ .

Which gives  $\frac{d\theta}{dt} = \frac{dv}{dt}$  .....(3.03)

But refractive index  $n = \frac{\text{Velocity in vacuum}}{\text{Velocity in medium}} = \frac{C}{V}$

\*And ultimately we have,  $\frac{dn}{dh} = \frac{1}{r}$  .....(3.04)

If we assume that the actual path of Figure 3.4a is replaced by a straight line path over the earth of modified effective radius  $a_e$  as in Figure 3.4b, then the distance  $\delta h$  must be same in both cases.

From fig.3.4b,  $(a_e+h)^2 + d^2 = (a_e+h+\delta h)^2$

$$\Rightarrow \delta h = \frac{d^2}{2(a_e+h)}$$

$$\approx \frac{d^2}{2a_e} \dots\dots\dots(3.05)$$

[\*Appendix B]

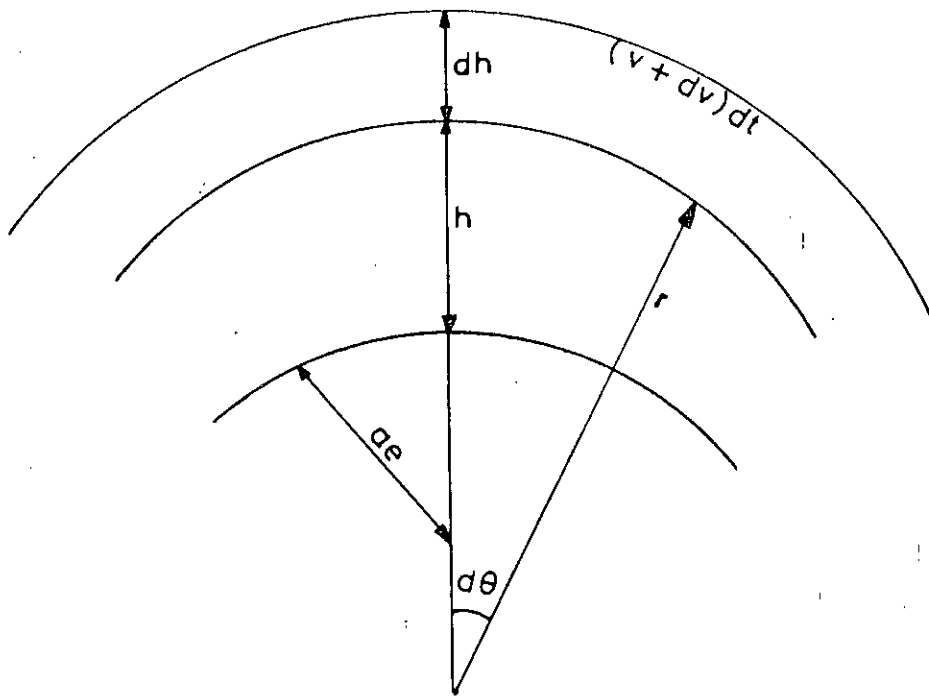


Fig.3.3 Illustration of refraction of tropospheric wave

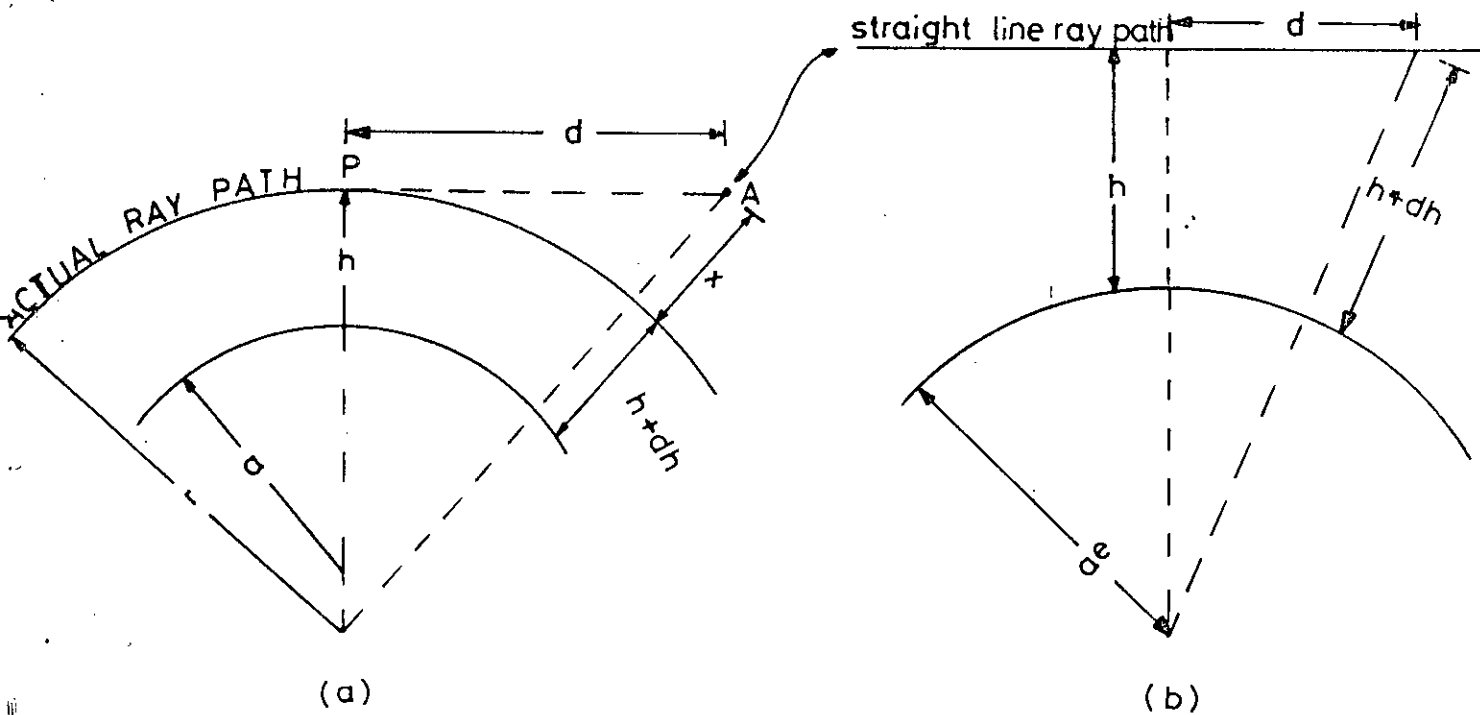


Fig.3.4 Illustration of equivalent ray paths over earth  
 (a) True radius 'a', (b) Modified radius  $a_e$ .

From fig.3.4a,  $(a_e+h)^2+d^2=(a+h+\delta h+x)^2$

$$\Rightarrow \delta h = \left( \frac{d^2}{2a} - x \right) \dots \dots \dots (3.06)$$

$$\Rightarrow \delta h = \frac{d^2}{2a} - \frac{d^2}{2r}$$

Hence  $\frac{1}{a_e} = \frac{1}{a} - \frac{1}{r}$

$$\Rightarrow \frac{1}{a_e} = \frac{1}{a} + \frac{\delta n}{\delta h}$$

Taking  $a_e=ka$

$$k = \frac{1}{1+a \frac{dn}{dh}} = \frac{1}{1-a/r} \dots \dots \dots (3.07)$$

But refractive index  $\left( \frac{\delta n}{\delta h} \right)$  Corresponding to standard atmospheric conditions is  $-0.039 \times 10^{-6}/\text{meter}$  and taking  $a=6,370 \text{ km}$  we get  $k=4/3$ .

### 3.3 RANGE OF SPACE-WAVE PROPAGATION:

Neclecting the effect of refraction of troposphere the maximum range of transmission of a signal through space wave

propagation is the line-of-sight distance as shown in figure 3.5. Hence elevation of antennas determines the range.

Considering the transmitting and receiving antenna heights are  $h_1$  and  $h_2$  respectively and 'a' is the radius of earth. But for propagation studies a standard index-of-refraction profile is commonly chosen such that it is equivalent to increasing the radius of earth by a factor 4/3 as find out in previous article. Thus we can use  $a_e$  instead of 'a'.

From the geometry of figure 3.5 we have,

$$R^2 + a_e^2 = (a_e + h_1)^2$$

$$\Rightarrow R^2 = h_1^2 + 2a_e h_1$$

But  $a_e \gg h_1$  and the slant distance R is nearly equal to the horizontal distance  $d_T$  to the horizon.

$$d_T^2 = 2a_e h_1$$

$$\Rightarrow d_T = (2a_e h_1)^{0.5} \dots\dots\dots(3.08)$$

If  $d_T$  is expressed in miles and  $h_1$  in feet we have,

$$d_T = (2h_1)^{0.5} \dots\dots\dots(3.08a)$$

Taking 'a'=3960 miles the maximum line-of-sight distance in miles between two antennas at height  $h_1$  and  $h_2$  feet above a spherical



earth with standard refraction condition is then readily seen to be given by

$$d_M = (2h_1)^{0.5} + (2h_2)^{0.5} \text{ (miles)} \dots\dots\dots(3.08b)$$

This may be put as

$$d_M = 4.12 [ (h_1)^{0.5} + (h_2)^{0.5} ] \text{ (km)} \dots\dots\dots(3.08c)$$

where  $h_1$  and  $h_2$  are in meters.

### 3.4 GENERAL FEATURE OF INTERFERENCE PHENOMENON WITH ANTENNAS LOCATED OVER SPHERICAL EARTH

The antennas located over a spherical earth with an effective earth radius  $a_e$  to account for standard refraction, it is very difficult to derive the formulas for interference effect. The indirect wave is now reflected from a curved surface, and its energy is diverged more than in the case when it is reflected from a flat earth [1,5,6]. This means that the ground-reflected wave reaching the receiver will be weaker than for a flat earth by the divergence factor  $D$  [1,15], which is less than unity. The grazing angle ( $\psi$ ) which is relative to the tangent plane at the point of reflection plays an important role in order to evaluate the reflection co-efficient.

The appropriate expression for the path gain factor  $F$  becomes

$$F = | 1 + D e^{j\psi} e^{-jko} \Delta R |$$

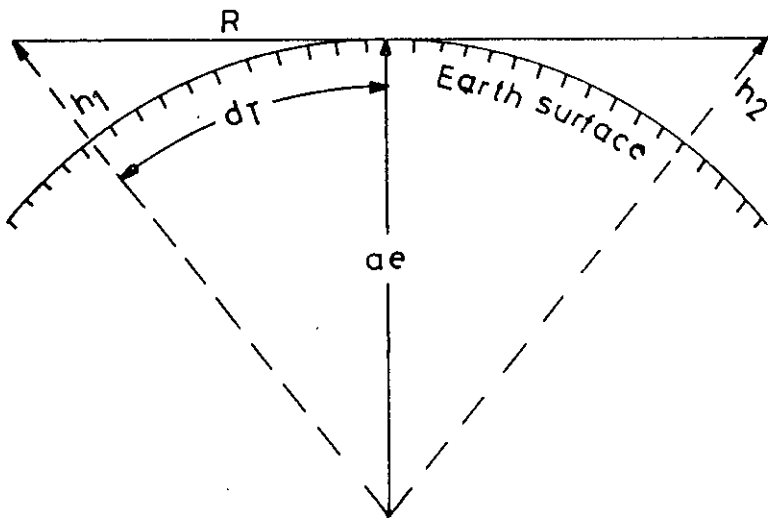


Fig.3.5 Illustration of horizontal range

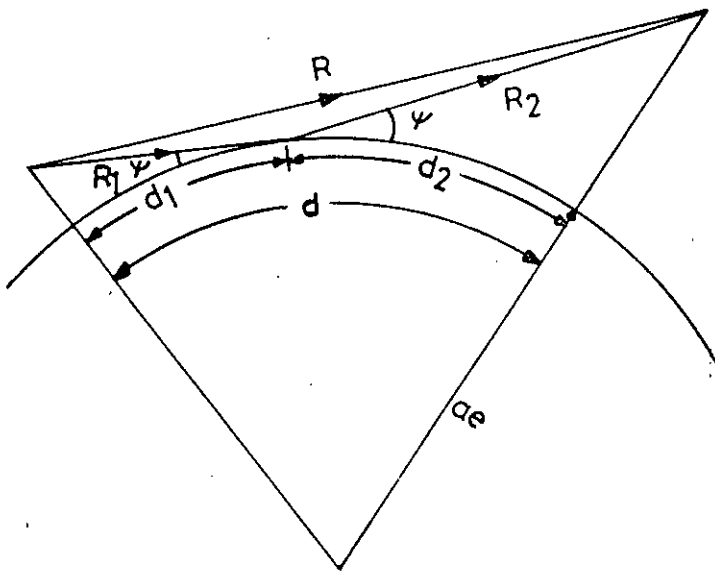


Fig.3.6 Illustration of reflection from a spherical earth.

$$\Rightarrow F = [(1+D)e^{\psi} - 4De^{\psi} \sin^2 \frac{\Phi - k_0 \Delta R}{2}]^{1/2} \dots\dots\dots(3.09)$$

where D is the ray-amplitude divergence factor and  $\Delta R$  is the path-length difference.

Here the known parameters are the two antenna heights  $h_1$  and  $h_2$  and the total range d. The point of reflection, which determines  $d_1, d_2$ , the grazing angle and the divergence factor D, is governed by a cubic equation. The new parameters J and K introduced here which are the functions of known parameter S and T.

$$\text{Path-length difference } \Delta R = R_1 + R_2 - R \dots\dots\dots(3.10)$$

$$\Delta R = \frac{2h_1 h_2}{d} J(S, T) \dots\dots\dots(3.11)$$

$$\tan \psi = \frac{h_1 + h_2}{d} K(S, T) \dots\dots\dots(3.12)$$

$$\text{Divergence factor } D = [1 + \frac{4S_1 S_2^2}{S(1-S_2)^2(1+T)}]^{0.5} \dots\dots\dots(3.13)$$

$$\text{where } S_1 = \frac{d_1}{(2a_e h_1)^{0.5}} \quad \text{and} \quad S_2 = \frac{d_2}{(2a_e h_2)^{0.5}}$$

$$S = \frac{d}{(2a_e h_1)^{0.5} + (2a_e h_2)^{0.5}}$$

$$\Rightarrow S = \frac{S_1 T + S_2}{1 + T}$$

$$T = (h_1/h_2)^{0.5} < 1$$

$$J(S,T) = (1-S_1^2)(1-S_2^2)$$

$$K(S,T) = \frac{(1-S_2^2) + T^2(1-S_1^2)}{1+T^2}$$

Here T is chosen less than unity, So  $h_1$  is taken as the height of the lowest antenna. The range  $d_1$  which determines  $d_2 = d - d_1$  and  $s_1, s_2$  may be found by solving the equations given below:

$$d_1 = \frac{d}{2} + p \cos\left(\frac{\phi + \pi}{3}\right) \dots\dots\dots(3.14)$$

$$\text{where } P = \frac{2}{\sqrt{3}} \left[ a_e (h_1 + h_2) + \frac{d^2}{4} \right]^{0.5} \dots\dots\dots(3.15a)$$

$$\phi = \cos^{-1} \left[ \frac{2a_e (h_1 - h_2) d}{P^3} \right] \quad h_1 \leq h_2 \quad \dots\dots\dots(3.15b)$$

The phase difference between the direct and reflected ray is given by

$$K_o \Delta R = \frac{2k_o h_1 h_2}{d} (1-S_1^2)(1-S_2^2)$$

$$= \frac{4\pi h_1}{(2a_e)^{0.5} \lambda_o} \frac{h_2/h_1}{d/d_T} (1-S_1^2)(1-S_2^2)$$

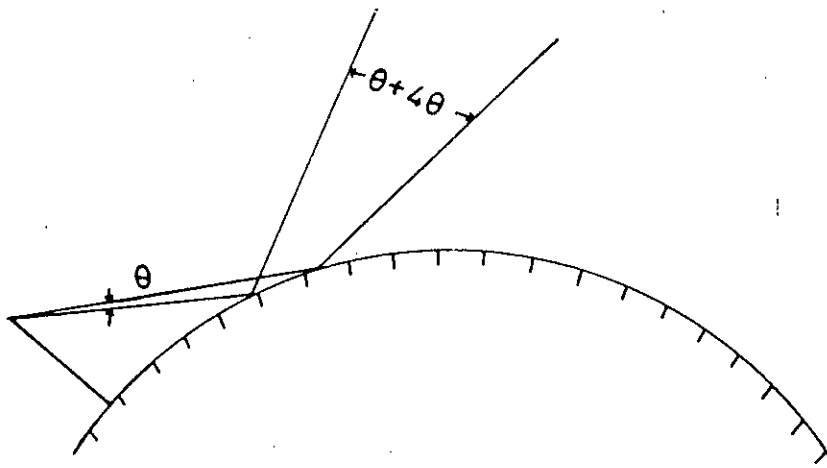


Fig.3.7 -Illustration of ray divergence upon reflected from a spherical surface.

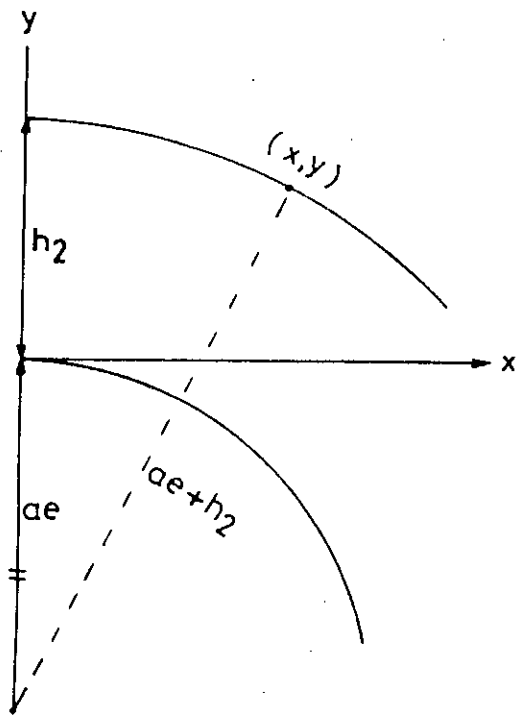


Fig.3.8 Illustration of constant height curve.

$$K_o \Delta R = V \sqrt{f} \dots \dots \dots (3.16a)$$

$$\text{where } V = \frac{4h_1^{3/2}}{(2a_e)^{0.5} \lambda_o} \dots \dots \dots (3.16b)$$

$$\text{and } f = \frac{h_2/h_1}{d/d_T} (1-S_1^2)(1-S_2^2) \dots \dots \dots (3.16c)$$

with  $d_T = (2a_e h_1)^{0.5}$ .

### 3.5 PATTERNS OF COVERAGE DIAGRAM

To draw the final pattern of coverage diagram the following constant curves contours must be drawing. They are as follows :

- i) Constant height curve
- ii) Constant values of divergence factor curve
- iii) The path-difference phase variable.
- iv) Curve F vs.  $d/d_T$  which supplies data for constructing a coverage diagram
- v) Final coverage diagram.

#### 3.5.1 CONSTANT HEIGHT CURVE

Plotting constant-height contours above the earth surface we consider the curve shown in fig.3.8. The constant height  $h_2$

above the earth surface and hence we have

$$(y+a_e)^2 - x^2 = (a_e+h_2)^2$$

$$\Rightarrow y^2 + 2a_e y + x^2 = h_2^2 + 2a_e h_2$$

Since  $y \ll a_e$  and  $h_2 \ll a_e$  we easily get

$$y = h_2 - \frac{x^2}{2a_e} \dots\dots\dots(3.17a)$$

which is a parabola. We can express it in normalize form as.

$$\frac{y}{h_1} = \frac{h_2}{h_1} - x^2/d_T^2$$

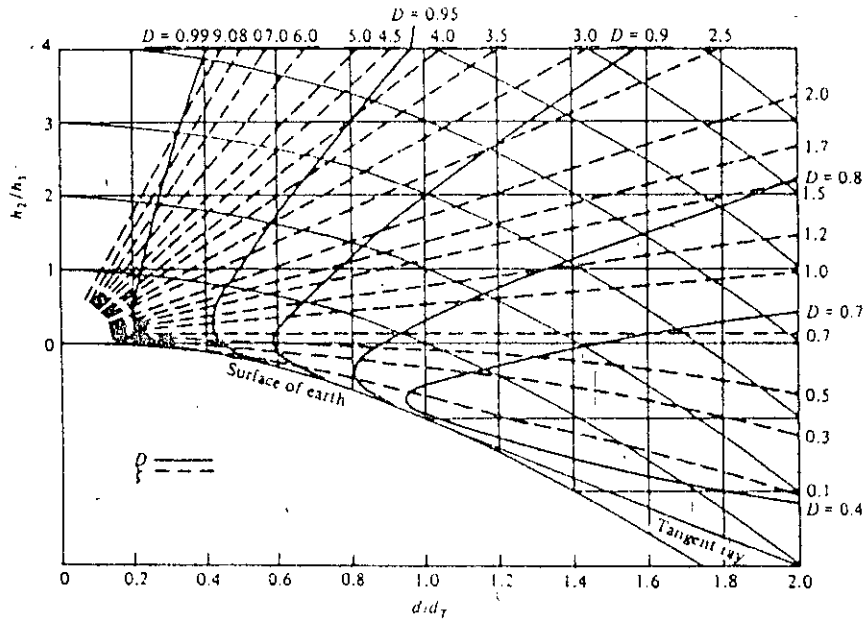
$$\Rightarrow \bar{y} = \frac{h_2}{h_1} - \bar{x}^2 \dots\dots\dots(3.17b)$$

where  $\bar{x} = x/d_T$  and  $\bar{y} = y/h_1$

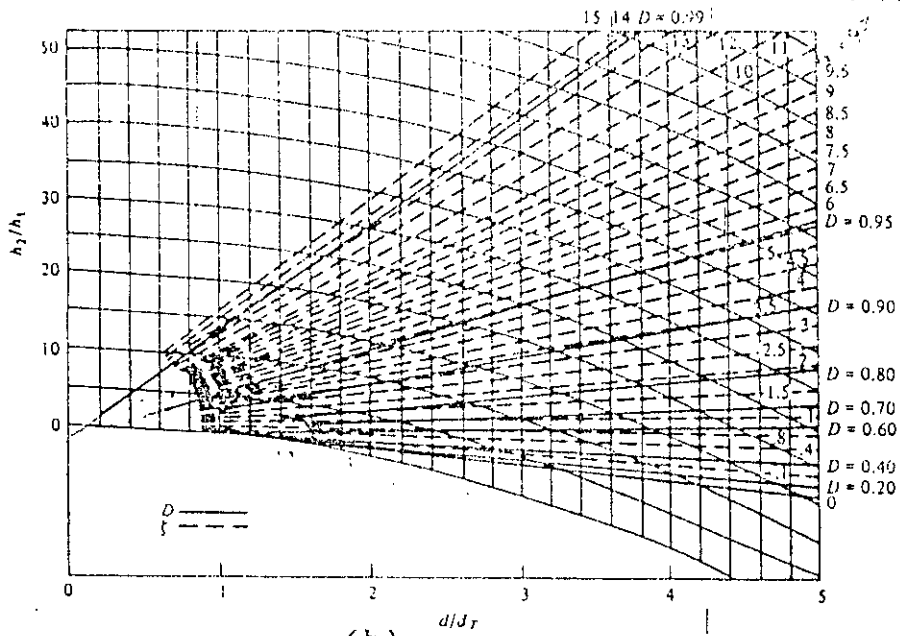
When the scale length of  $y$  changes relative to  $x$  then the shape of the parabolic curves changes.

### 3.5.2 CONSTANT VALUES OF DIVERGENCE FACTOR CURVE AND THE PATH DIFFERENCE PHASE VARIABLE CURVES

The constant values of divergence factor curve and the path-length phase-difference factor curve can be plotted by taking a series of values using the equation from 3.10 to 3.16. Such plots on curvilinear grid in which the horizontal co-ordinate is  $d/d_T$



(a)



(b)

Fig. 3.9 Contours showing constant values of divergence factor  $D$  and the path difference phase variable  
 (a) Contours for the value  $h_2/h_1$  up to 4  
 (b) Contours for the value  $h_2/h_1$  up to 50  
 (These figures have been taken from reference 1)



and vertical co-ordinate is  $h_2/h_1$  shown in the figure 3.9. These curves supply the values of divergence factor and path difference phase variable to calculate path gain factor using formula 3.09.

### 3.5.3 PATH GAIN FACTOR CALCULATION TO DRAW THE THE CURVE F vs. $d/d_T$

The path gain formula derived in section 3.04 is given.

$$F = [(1 + D \cos^2 \theta - 4D \cos^2 \theta \sin^2 \frac{\theta - k_0 \Delta R}{2})]^{0.5} \dots \dots \dots (3.09)$$

is a function of  $h_2/h_1$  and  $d/d_T$ . Since D and  $\theta$  depend on these parameters. If we choose a lobe corresponding to free-space range of  $2d_T$ , then the maximum value  $X=d/d_T$  can achieve will be 4 when  $D=1$  and we located in a lobe maximum.

For other values of D and  $\theta$  we have

$$x = \frac{d}{d_T} = 2F \dots \dots \dots (3.18)$$

while for a free-space range of  $\sqrt{2}d_T$  and  $d_T$ ,  $x=\sqrt{2} F$  and  $x=F$  respectively. To draw the curve F vs.  $d/d_T$  we compute F as a function of  $d/d_T$  for several values of  $h_2/h_1$ . We must follow the procedure as followed in flat-earth formula.

$$F = m \frac{d}{d_T} = \frac{d/d_T}{r_f/d_T}$$

$$\Rightarrow \frac{d}{d_T} = (r_F/d_T) F\left(\frac{d}{d_T}, \frac{h_2}{h_1}\right) \dots\dots\dots(3.19)$$

If we choose the reflection co-efficient approximately equal to -1 then the path gain formula becomes

$$F = [(1+D)^2 - 4D \cos^2(\psi/2)]^{0.5} \dots\dots\dots(3.20)$$

gives the values of F vs.  $d/d_T$  curves which supplies the data for constructing final coverage diagram. Taking the reflection co-efficient as -1 the coverage diagram is drawn in the figure 3.10 and 3.11. When the reflection co-efficient differs significantly from -1 then the coverage diagram describing the path gain factor F for that particular case must be constructed. The parameter D and  $\xi$  may still be found from Fig. 3.09a and 3.09b, but now the grazing angle  $\psi$  must also be found in order to determine the reflection co-efficient. The tangent ray also be constructed which is a straight line intersects the  $h_2/h_1$  curve at  $d/d_T = 1 + (h_2/h_1)^{1/2}$ . One can draw F vs.  $d/d_T$  curve either using flat-earth formula beyond the values  $\xi$  and D as shown in figure 3.9 or directly by the simple FORTRAN program as discussed in appendix C. Precaution must be follow when constructing coverage diagram in the region of diffraction zone i.e the region close to tangent ray is approached.

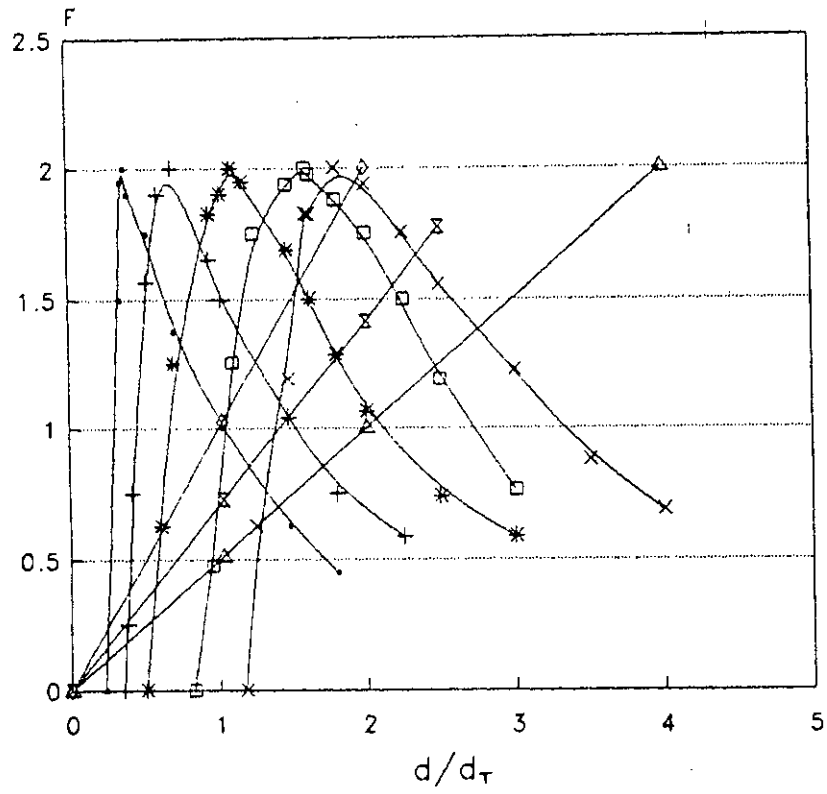


Fig.3.10 Data for constructing a coverage diagram for  $v=.268$

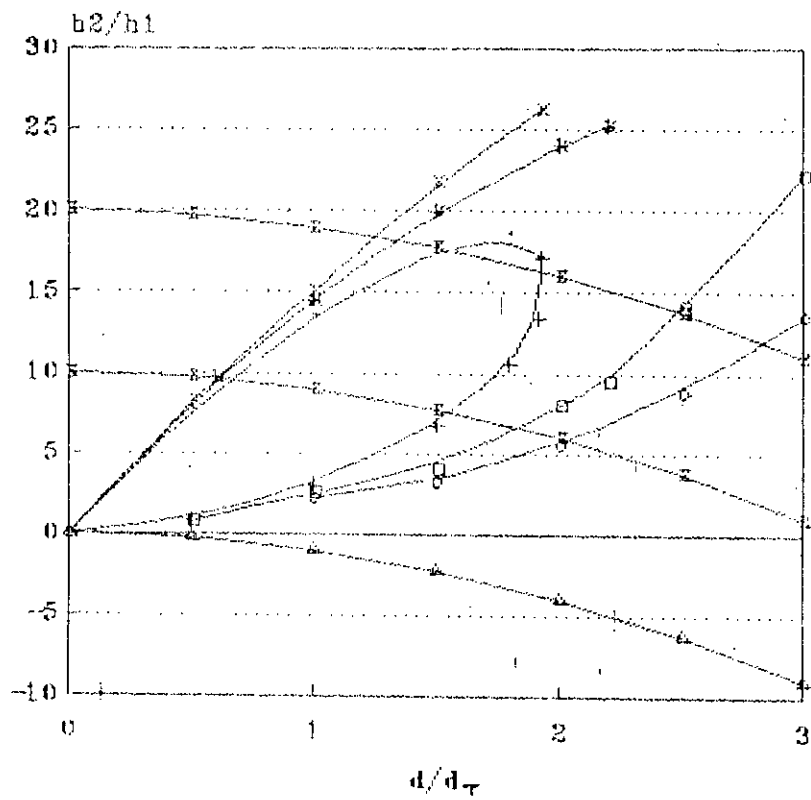


Fig.3.11 Coverage diagram for  $v=0.268$  based on data in figure 3.10.

3.5.4 STEPS INVOLVED TO CONSTRUCT A COVERAGE DIAGRAM ARE AS FOLLOWS

- a) To calculate the parameter  $v$
- b) Then to calculate  $v_f$
- c) To draw the tangent ray
- d) To draw  $F$  vs.  $d/d_T$  curve
- e) To draw final coverage diagram.

3.6 THE FIELD IN THE DIFFRACTION ZONE

Due to diffraction effects the radiated field penetrates into the shadow zone below the tangent ray although the field strength below the tangent ray will be zero according to the optics [1,11,18]. The field strength is influenced by diffraction effect in the region above and very close to the tangent ray. The field strength calculation in the vicinity of the tangent ray is thus complex and labourious. The simple procedure to calculate the value of  $d/d_T$  in the diffraction by putting  $\pi v/2 = \pi/2$  for first maximum and  $F = 1+D$  and  $F = (1+D)^{1/2}$  where  $\pi v/2 = \pi/4$ . Joining these by a smooth curve and several values of  $F$  is determined in the vicinity of diffraction zone for several values of  $d/d_T$ .

There is a formula to calculate  $F$  express as

$$F = V(X)U(Z_1)U(Z_2) \dots\dots\dots(3.21)$$

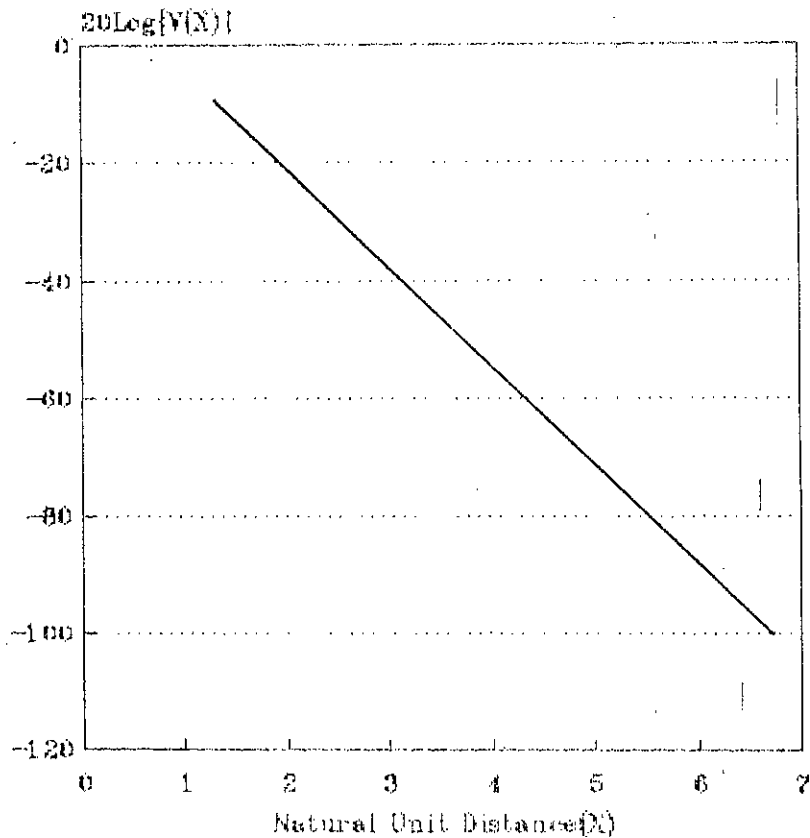


Fig.3.12 A typical plot of attenuation function  $V(X)$  (in dB) against distance  $(X)$

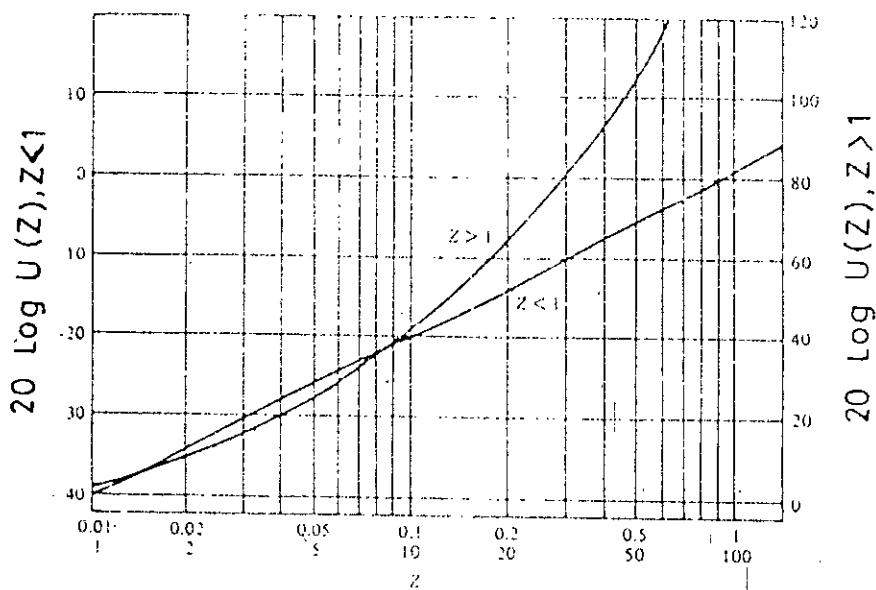


Fig.3.13 Illustration of the height gain function  $U(Z)$   
 ( This figure has been taken from reference 1 )

where  $V(X)=2(\pi X)^{0.5}e^{-2.02X}$  the main attenuation factor, and X is the distance measured in natural unit of L and Y and Z are the antenna heights measured in natural unit of height H. These are given by

$$L = 2(a_e/4K_0)^{1/3} = 28.41 \lambda_0^{1/3} \text{ (km)} \dots\dots\dots(3.22a)$$

$$H = (a_e/2k_0)^{1/3} = 47.55 \lambda_0^{2/3} \text{ (m)} \dots\dots\dots(3.22b)$$

where  $\lambda_0$  is measured in meters  $X = d/L$ ,  $Z_{1,2} = h_{1,2}/H$  in natural unit. The incident power per unit area at the receiving terminal will be expressed by the following equation.

$$P_{in} = \frac{P_T G}{4\pi d^2} \left( \frac{F d_T}{d} \right)^2 \dots\dots\dots(3.23)$$

It is then easy to plot the curve  $20 \log F - 20 \log(d/d_T)$ . Every doubling of d beyond the point  $d/d_T$  the value is simply a reduction by 6 dB from  $20 \log F$ . The path gain factor should be plotted as a function of  $d/d_T$  shown in figure 3.14. The calculating procedure of path gain factor is as follows :

- (i) To calculate v
- (ii) To calculate  $\pi \xi$  for maximum F and point of quarter of F
- (iii) To calculate d in term of  $d_T$  using the curve 3.09a
- (iv) To choose the diffraction zone in term of  $d_T$
- (v) To calculate X ( With the help of Fig. 3.12)

(vi) To calculate Z ( With the help of Fig. 3.13)

Putting the above calculating values of X and Z in equation 3.21 F may be calculated.

### 3.7 MIDPATH-OBSTACLE DIFFRACTION LOSS

The midpath obstacles such as tall land (earth bulgs), trees, tall buildings, hills etc. partially block the propagation path as a result field loss occur [1,3,6,18]. The effect of the hill can be modeled as a thin plane having the same clearance distance  $h_c$  from the line-of-sight path, provided there is no specular reflection from the top of the hill. (shown in figure 3.15). The thin plane model also shown in figure 3.16. It is very complex to compute the diffraction loss when the reflected field is diffracted by knife-edge.

Analyzing the figures 3.15 the clearance height is given by

$$h_c = \left( \frac{d_2 h_1 + d_1 h_2}{d} - h \right) \cos \theta_c \dots \dots \dots (3.24)$$

where h is the height of obstruction.

There is a solution named optical phenomena which deals with the Fresnel surface. The nth Fresnel surface is that for which the sum of distances between transmitter and receiver and a point on the surface of the ellipsoid of revolution exceeds by  $n\pi/2$ , the distance between transmitter and receiver. To avoid



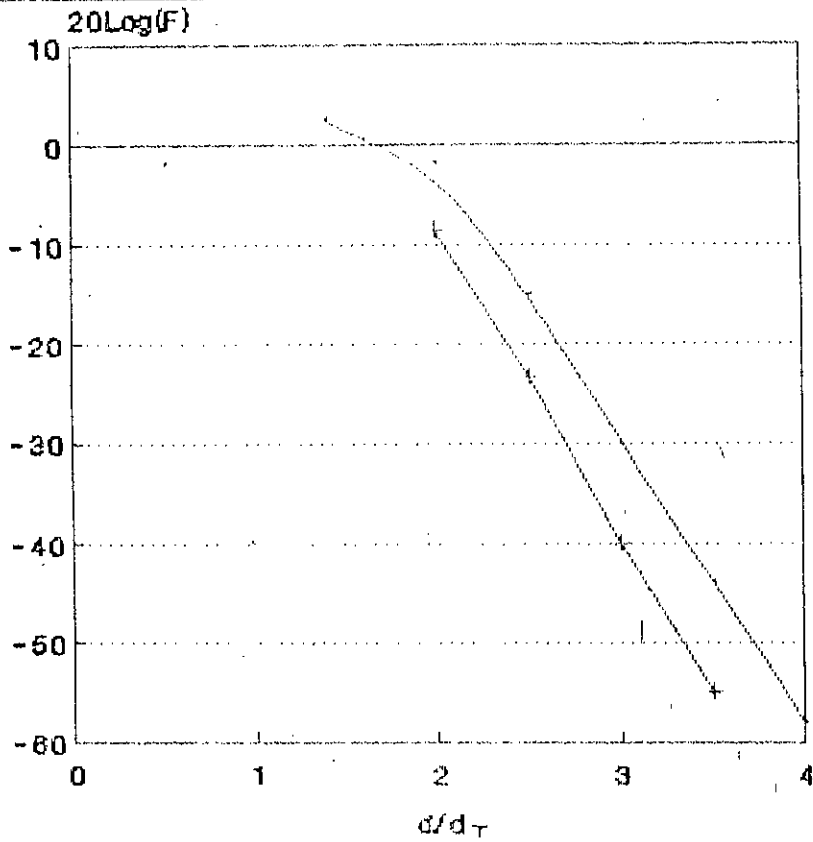


Fig.3.14 Path gain factor  $F$  in dB for  $h_1=24\text{m}$ ,  $h_2=60\text{m}$ ,  $f=3\text{GHz}$

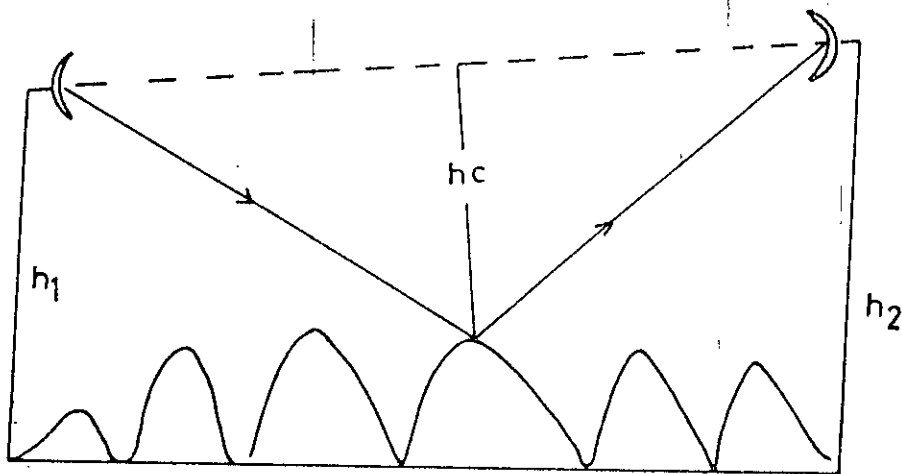
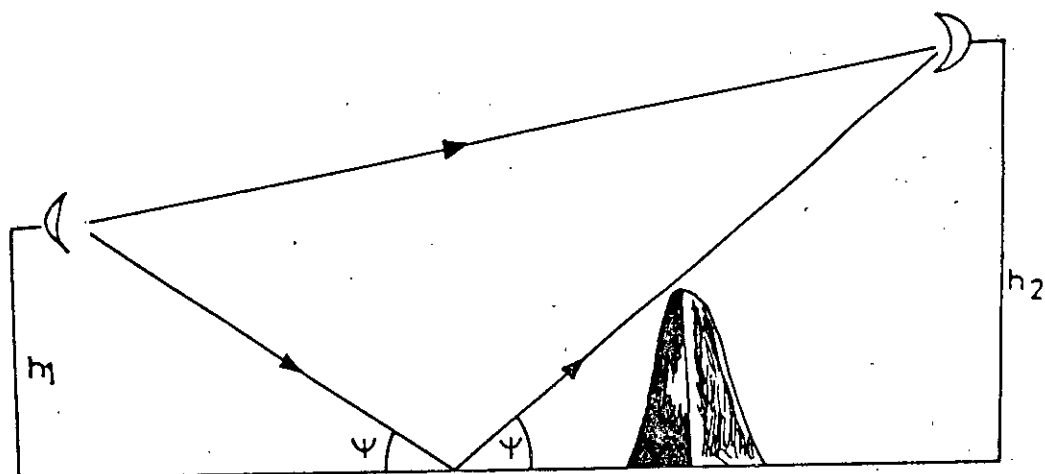
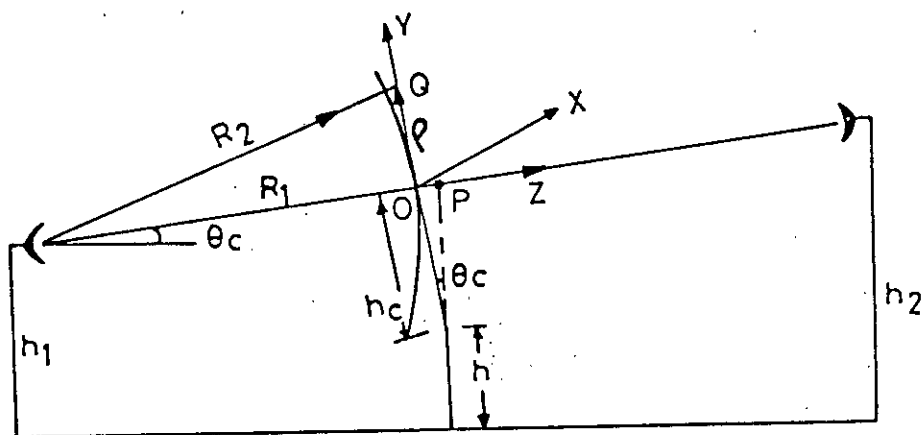


Fig.3.15 Illustration of midpath obstacle



(a)



(b)

Fig.3.16--(a) Knife-edge model ( obstruction not blocking the reflected ray) .(b) Knife-edge model showing propagation parameters.

intervening obstacles the clearance between the direct ray and the highest obstacle should be sufficient to ensure that the difference between the path lengths of a reflected ray and the direct rays exceeds a half wavelength. The minimum clearance distance shown in the Fig.3.17 is the radius of the first Fresnel zone [1,3]. It is given by

$$H_1 = [\lambda d_1(1 - d_1/d)]^{0.5} \dots\dots\dots(3.25)$$

where d = total path length

$d_1$  = The distance from the transmitter.

The amount of additional clearance needed over an obstacle is found to be 0.6R.

where  $R=17.3(d_1d_2/f_d)^{0.5}$

$d_1$ =distance from transmitter

$d_2$ =distance from receiver

The path gain factor due to diffraction is given by

$$F_d = (1/2)^{0.5} \left| \int_{-h_c}^{\infty} e^{-j u^2/2} du \right| \dots\dots\dots(3.26)$$

where  $H_c = (2a/j\lambda)^{1/2}h_c$ . When  $h_c = 0$ , the above Fresnel integral equals  $0.5 (\pi/a)^{0.5}$  i.e. one half of the incident radiation blocked, which results in 6 dB loss.

The path gain profiles drawn using the above Fresnel integral caused by the knife-edge diffraction loss shown in the Fig.3.18.

Under normal (standard) atmospheric conditions the clearance can be determined by plotting the path profile above an earth with

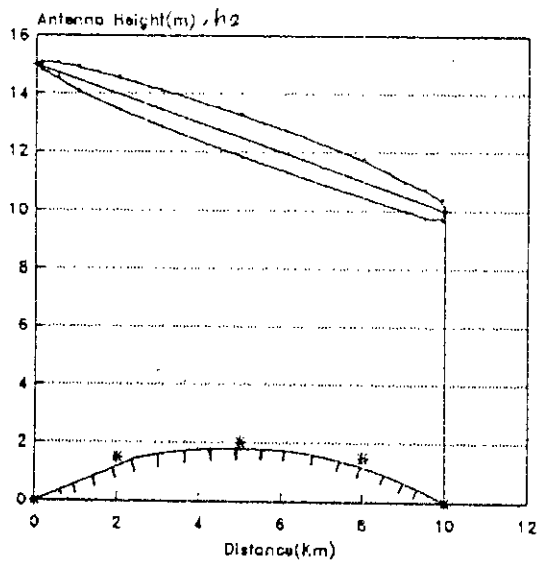


Fig.3.17 . Illustration of first Fresnel zone.

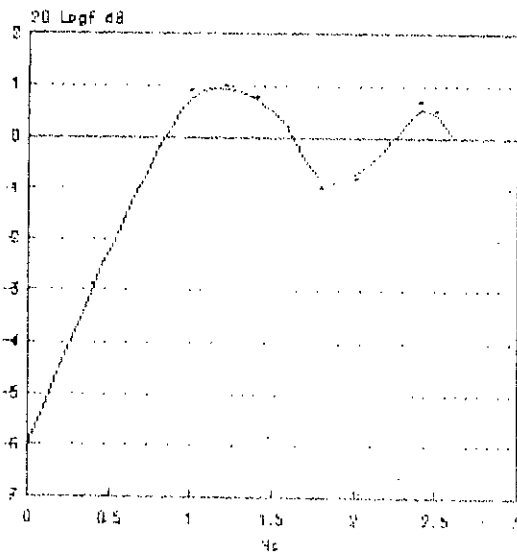


Fig.3.18 The path gain factor  $F_d$  caused by knife-edge diffraction loss in dB as a function of  $H_c$ .

effective radius equal to  $4/3$  the actual radius. If the refractive index is increased under some conditions the waves will then curve upward and thereby reduce the effective clearance. From Figure 3.18 it is cleared that path profile is drawn above an earth with effective radius the probability of fading owing to midpath obstacles diffraction loss will be negligible.

## CHAPTER 4

# MICROWAVE COMMUNICATION LINK PERFORMANCE CALCULATION

### 4.1 SYSTEM LINK MODEL

The general model of a mw link is shown in Figure 4.1. The signal is generated by the transmitter enters the feeder in which attenuation occurs. This attenuated signals enter the antenna and then transmitted. In the receiving side the receiving antenna received the signals. These signals pass through the feeder to the receiver input.

### 4.2 RADIO SYSTEM PERFORMANCE CALCULATION

The steps involved to evaluate the expected performance of a microwave channel are as follows:

- a) Noise requirement (Signal to noise ratio)
- b) Receiver noise figure and Noise power
- c) Required received carrier level
- d) System gain/(Link equation in dB)
- e) Diversity calculation (Fading)
- f) System performance.

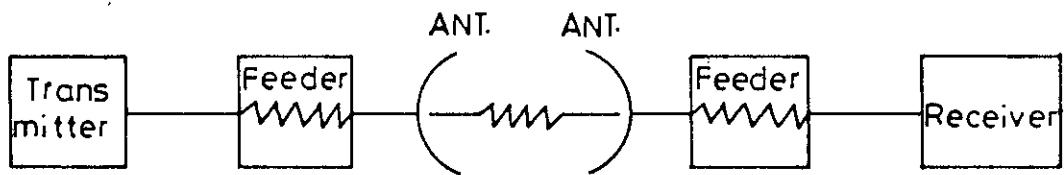


Fig.4.1 A microwave link model.

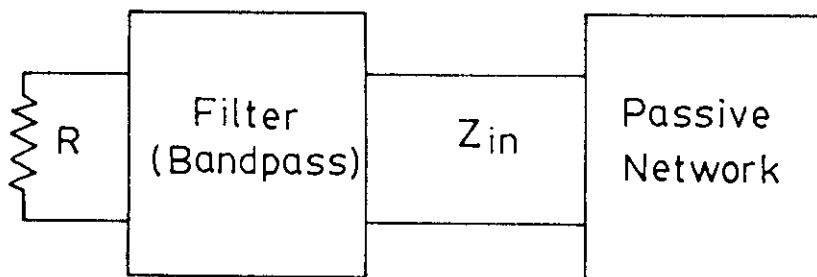


Fig.4.2 A resistor connected to a passive network.

11/1

### 4.3 NOISE REQUIREMENT

Any undesired signal in a communication circuit is called noise. The types of noise that occur in a communication system are as follows:

- a) Thermal noise
- b) Quantum noise
- c) Intermodulation noise
- d) Crosstalk noise
- e) Impulse noise.

#### 4.3.1 THERMAL NOISE

This type of noise occurs in all transmission and all communication equipment arising from the random electric motion. It is characterized by a uniform distribution of energy over the frequency spectrum. The random motion of electrons in a resistor  $R$  at an absolute temperature  $T$  exhibits a random noise voltage across its terminals. The power spectral density of this noise voltage is given by Planck's distribution law [1,6,16,17]

$$P_n = \frac{4hfRB_n}{e^{hf/KT}-1} \dots\dots\dots (4.01)$$

where  $h$  is plank's constant =  $6.6254 \times 10^{-34}$  Joules-sec.



k is Boltzmann's constant =  $1.38 \times 10^{-23}$  J/°K

R is the resistance (ohm)

f is the frequency (Hz)

$B_n$  is Band width in which noise is observed

According to the Nyquist's formula the mean square value of generated noise voltage is given by

$$e_n^2 = 4kTB_nR \dots\dots\dots(4.02)$$

Thermal noise is termed as white noise referring to the average uniform spectrum distribution of energy with respect to frequency. It is independent of frequency over the bandwidth.

Let a resistor R be connected to a one-port network, as shown in Figure 4.02. We also assume that an ideal narrow-band lossless filter is inserted between R and the network. The resistor R will deliver thermal noise to the network in a narrow band of frequency  $B_n$  centered of f. At system thermodynamic equilibrium the network must deliver an equal amount of noise power to R at the same frequency. The use of a lossless narrow band filter is simply a method used to demonstrate that the flow of noise energy from R to the network and from network to R must balance at each frequency.

#### 4.3.2 QUANTUM NOISE

At high frequencies where  $hf > kT$  such as used in optical communication the thermal noise spectrum eventually drops to zero. But a quantum noise term equal to  $hf$  is added that to give inherent noise limitation at all frequencies.

#### 4.3.3 INTERMODULATION NOISE

It is the results of the presence of intermodulation products. The products result where two or more signal mixed together while passing through a nonlinear device.

It may results from number of causes:

- i) Improper level setting i.e. two high level input to a device derives it into nonlinear operating region.
- ii) Improper alignment causing the device to function non-linearity.
- iii) Non linear envelope delay

#### 4.3.4 CROSSTALK NOISE:

Gross talk interference can be caused by unwanted coupling between two signal due to capacitance, leakage or mutual

inductance of lines. Low level cross talk can be intelligible and give the user the impression of a lack of secrecy. When cross talk energy is transferred from one channel to another it can usually be detected at each end of the disturbed channel as shown in figure 4.03. When the cross talk is propagated over the disturbed channel in the same direction as its own signal, the cross talk is called far-end cross talk. When it is in the opposite direction is called near-end crosstalk.

#### 4.3.5 IMPULSE NOISE

It is non-continuous type of noise. It consists of irregular pulses or spikes of noise of short duration and of relatively high amplitude for voice telephone.

#### 4.3.6 SIGNAL TO NOISE RATIO (S/N)

It is the amount by which a signal level exceeds its corresponding noise level. In  $dB_m$  the S/N ratio is equal to the difference between the level of signal in  $dB_m$  to the level of noise in  $dB_m$ .

#### 4.4 NOISE FIGURE AND NOISE TEMPERATURE

In a system all network whether passive or active and all transmission media contribute noise to transmission system. Noise Figure is a measure of noise produced by the practical system compared to an ideal network [1,8,11,16].

System noise figure NF is defined as

$$\begin{aligned}
 NF &= \frac{(S/N)_{in}}{(S/N)_{out}} \\
 &= \frac{S_{in} N_{out}}{S_{out} N_{in}} \dots\dots\dots(4.04a)
 \end{aligned}$$

But  $N_{in} = KTB_n$  and  $S_{out}/S_{in} = G$  (Gain)

$$\Rightarrow NF = \frac{N_{out}}{KTB_n G} \dots\dots\dots(4.04b)$$

In deceibel unit,

$$(NF)_{dB} = 10 \log(N_{out}) - 10 \log(KTB_n G) \dots\dots\dots(4.05)$$

For conventional noisy receivers the concept of noise figure is enough to describe their performance. But for low noise receivers a more useful measure receiver noise is the effective input noise temperature ( $T_r$ ) of the receiver [1,8,11,16]. Now consider the equivalent noisy transducer shown in figure 4.4.

From equation 4.04b we can express noise figure as

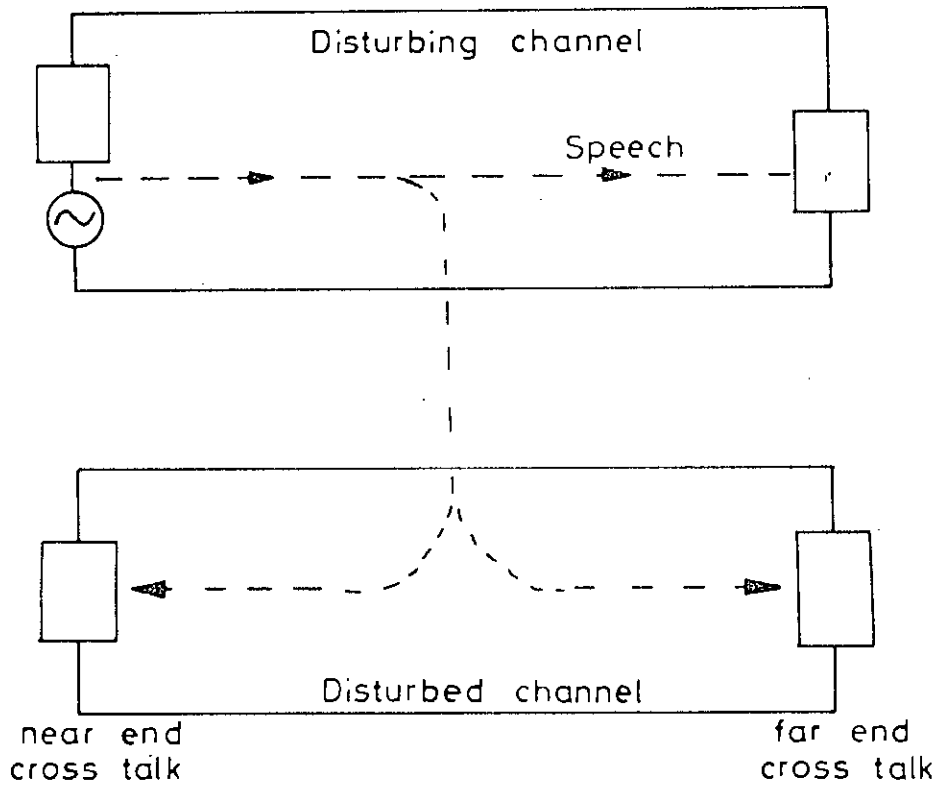


Fig.4.3- Illustration of cross talk noise.

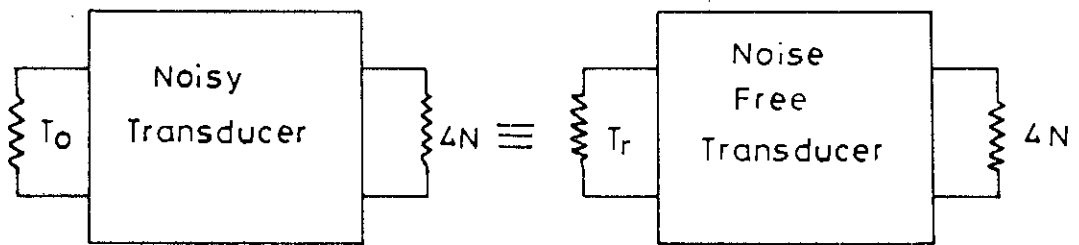


Fig.4.4 Equivalent noise free transducer model of a noisy transducer.

$$NF = \frac{N_{out}}{KTGB_n}$$

$$= \frac{KT_0GB_n + \Delta N}{KTGB_n}$$

where  $\Delta N = KT_rGB_n$

Hence 
$$NF = \frac{KT_0GB_n + KT_rGB_n}{KT_0GB_n}$$

$$\Rightarrow T_r = (NF - 1)T_0 \dots\dots\dots(4.06)$$

Then  $T_r$  referred to the input terminal is a term which characterizes the noiseless of a given receiver.

#### 4.5 REQUIRED RECEIVED CARRIER LEVEL

The required received carrier level for a minimum quality objective is defined

$$C_{min} = P_T - G_S \dots\dots\dots(4.07)$$

where  $C_{min}$  = received carrier level (dB<sub>m</sub>) for a minimum quality objective; it is called receiver threshold.

$P_T$  = transmitter output power (dB<sub>m</sub>), excluding antenna branching network

$G_S$  = system gain in dB.

## 4.6 LINK EQUATION AND SYSTEM GAIN

### 4.6.1 LINK EQUATION

An isotropic antenna radiates power in all direction. But an directional antenna radiates power for particular direction. If  $P_T$  is the average power radiates from an antenna in all direction we get the radiate power per unit area as

$$P_{Di} = \frac{P_T}{4\pi d^2} \dots\dots\dots(4.08)$$

where  $d$  is the link range.

But all practical antenna are somewhat directional that is power density along the direction of maximum deviation is

$$\begin{aligned} P_D &= P_{Di}G_T \\ &= \frac{P_T G_T}{4\pi d^2} \dots\dots\dots(4.09) \end{aligned}$$

where  $G_T$  is the maximum density of gain.

Receiving power  $P_R$  can be expresse as

$$P_R = P_D A_{eff} \dots\dots\dots(4.10a)$$

Where  $A_{eff}$  is effective area of receiving antenna.

$$\Rightarrow P_R = \left( \frac{P_T G_T}{4\pi d^2} \right) A_{eff} \dots\dots\dots(4.10b)$$

But effective area can be expressed as

$$A_{\text{eff}} = G_R \lambda^2 / 4\pi \quad \dots\dots\dots(4.10c)$$

Where  $G_R$  is the directivity gain of receiving antenna,

$\lambda$  is the wave length.

Hence 
$$P_R = \frac{P_T G_T G_R \lambda^2}{(4\pi d)^2} \quad \dots\dots\dots(4.11)$$

In decibel unit we get the ratio of the receiving and the transmitting power

$$\begin{aligned} (P_R/P_T)_{\text{dB}} &= [ 10 \text{ Log } G_T G_R ] - [ 20 \text{ Log } 4\pi d ] + [ 10 \text{ Log } \lambda^2 ] \\ &= \text{EIRP} - L_{\text{dB}} \quad \dots\dots\dots(4.12) \end{aligned}$$

Where EIRP ( Effective Interference Radiate Power ) =  $[G_T G_R]_{\text{dB}}$

$L_{\text{dB}}$  = Line Loss

From equation 4.11 and 4.12 we have line loss as follows:

$$\begin{aligned} L_{\text{dB}} &= 32.5 + 20 \text{ Log } F + 20 \text{ Log } d \quad [ F \text{ in MHz, } d \text{ in Km } ] \\ &= 96.6 + 20 \text{ Log } F + 20 \text{ Log } d \quad [ F \text{ in GHz, } d \text{ in mile } ] \\ &\quad \dots\dots\dots(4.13) \end{aligned}$$

#### 4.6.2 SYSTEM GAIN

System gain is the useful measure of performance because it incorporates many parameters of interest to the designer of microwave system. Its value must be greater than or at least equal to the sum of the gains and losses which are external to



the equipment. From equation 4.07 we have the mathematical expression as follows:

$$G_S = P_T - C_{\min} \dots\dots\dots (4.07)$$

$$\Rightarrow G_S = L_{dB} + L_{Feed} + L_B - G_T - G_R \dots\dots\dots (4.14a)$$

Unfaded received power  $P_R$  ( $C_{\min}$ ) is given by

$$P_R = P_T + G_T + G_R - L_{dB} - L_{Feed} - L_B \dots\dots\dots (4.14b)$$

Where  $P_T$  = Transmitter output power

$G_T$  = Transmitting antenna gain

$G_R$  = Receiving antenna gain

$L_{dB}$  = Span loss

$L_{Feed}$  = Feeder loss

$B$  = Branching network loss

Receiver noise ( $N_0$ ) is given by.

$$N_0 = 10 \text{ Log } KTB + NF \dots\dots\dots (4.15)$$

Where  $NF$  is the receiver noise figure.

$$\text{Hence } S/N_0 \text{ (Signal to noise ratio)} = P_R - N_0 \dots\dots\dots (4.16)$$

Antenna Gain: The gain of a parabolic antenna can be calculated as

$$G = \eta \left( \frac{\pi D}{\lambda} \right)^2 \dots\dots\dots (4.17a)$$

Where  $\eta$  = Antenna efficiency (Typically 0.55-.60)

$D$  = Antenna diameter (Aperture Dia.)

$\lambda$  = Wave length

At 55% efficiency we can express G in dB as

$$G_{dB} = 20 \log D + 20 \log F + 17.8 \quad (D \text{ in m, } F \text{ in GHz}) \quad \dots(4.17b)$$

#### 4.7 UNFADED INTERFERENCE NOISE (S/I) CALCULATIONS

##### 4.7.1 INTERFERENCE OF AN ADJACENT CHANNEL (S/I)<sub>X</sub>

This source of interference is suppressed by cross polarization discrimination (CPD) of antenna, transmitted spectrum shaping and selectivity within the desired receiver.

$$(S/I)_{\text{unfaded}} = \text{CPD} + \text{IRF}(\text{CPD}) \quad \dots(4.18)$$

where CPD = Cross polarization discrimination of antenna.

IRF(CPD) = Interference reduction factor of this radio for the minimum frequency spacing between cross polarized adjacent channels.

##### 4.7.2 TRANSMITTER-RECEIVER INTERFERENCE S/I(X-R)

S/I(X-R) defines as the ratio of received power to the interference noise for the minimum frequency spacing between a transmitter and a receiver.

$$\frac{P_R}{\text{IRF}(X-R)} = P_T + L_B + L_{\text{Feed}(x)} + L_{\text{Feed}(x)} + D_{X-R} \quad \dots(4.19)$$

Where,  $P_R$  = Receiver Power

$P_T$  = Transmitter power

$L_B$  = Branching Network Loss

$L_{Feed}(X)$  = Transmitter Feeder Loss

$L_{Feed}(R)$  = Receiver Feeder Loss

$D_{X-R}$  = Transmitter-Receiver Decoupling

$IRF(X-R)$  = IRF for minimum frequency  
separation of  $T_X$  and  $R_X$ .

It is also possible front- to- back antenna interference. The design engineers must consider this case as well as the previous interference effect.

#### 4.8 FADE MARGIN REQUIREMENTS FOR A SPECIFIED SYSTEM AVAILABILITY

Fading is the fluctuation in transmitter line. Fading depends on temperature, pressure and humidity of air. The effect of fading on operational unavailability can be minimised by space or frequency diversity techniques. Both of these techniques are based on the hypothesis that simultaneous fading on both radio transmission paths is unlikely. The hop fade margin (dB) of non-diversity system (FM) can be solved from the following equation:

$$FM = 30 \log(d) + 10 \log(6ABf) - 10 \log(1-R) - 70 \quad \dots\dots\dots(4.20)$$

where A = Roughness factor

= 4 for very smooth terrain

= 1 for average terrain with some roughness

= ¼ for mountainous, very rough terrain

B = factor to convert worstmonth probability to annual probability

= ½ for Great Lakes or similar hot, humid areas

= ¼ for average inland areas

= 1/8 - for mountainous or very dry areas

1-R = Reliability objective for a 400 km route

It may be used on a worst-month basis by setting B=1, we may obtain the fade margin for an unprotected utility having 99.99% service reliability per hop.

$$\Rightarrow (1-R) = 0.01\% = 0.0001$$

$$FM = 30 \log(d) + 10 \log(6A) + 10 \log f - 30 \text{ dB} \quad \dots\dots\dots(4.21)$$

The system gain equation (equation no. 4.14) considering FM we can express as,

$$G_S \geq FM + L_{dB} + L_{FEED} + l_B - g_t - G_R \quad \dots\dots\dots(4.22a)$$

which becomes,

$$G_s = 50 \log d + 30 \log f + 10 \log(6A) + 62.4 + L_{FEED} + L_B - G_T - G_R \dots (4.22b)$$

#### 4.9 PARAMETERS FOR SYSTEM PERFORMANCE

Considering the system performance the estimated parameters are as follows:

- i) Frequency
- ii) Hop distance
- iii) Tower heights
- iv) Antenna diameter
- v) Transmitting power
- vi) Receiver threshold

Calculating parameters are:

- i) Free space loss
- ii) Antenna gain
- iii) Noise Figure
- iv) Feeder Loss
- v) Branching Network Loss
- vi) Received Power
- vii) Noise
- viii) Threshold S/N
- ix) S/I ratio
- x) Fade margin of S/N, S/I.

# CHAPTER 5

## CALCULATION FOR A MICROWAVE LINK IN BANGLADESH

### 5.1 INTRODUCTION

This chapter deals with the verification of interference patterns calculation which are discussed in the previous chapter for microwave communication link. This is devoted to a treatment of a microwave communication link in Bangladesh. Available datas are taken from Bangladesh T & T Board and specified results have been obtained for a UHF and a SHF links.

### 5.2 CALCULATION OF AN UHF LINK

This section deals with the performance calculation of an UHF link of Bangladesh.

#### 5.2.1 DATAS AND PARAMETERS

Transmitting Antenna Height	...60.0	m
Hop Distance	.....25.0	km
Antenna Diameter	.....1.2	m
Transmitting Power	.....30.0	dBm
Transmitting Frequency	.....1.5	GHz
Noise Threshold	.....4.5	dBm(max.)
Receiving Power	.....From -25.0	dBm to -40.0 dBm
Branching Loss	.....4.5	dB

#### 5.2.2 PATTERNS OF COVERAGE DIAGRAM

Using the formula 2.11 for the datas mentioned above we can draw the constant  $F/r$  curve in the  $h_2$ - $d$  plane which is the coverage diagram. Such a diagram is shown in the fig.5.1. In

the first lobe the receiving antenna height is 22 m at the span distant 25 km which is very close to the height calculated by the Fujitsu Ltd., Tokyo, Japan for UHF link for Bangladesh. The coverage diagram in spherical earth phenomena is also shown in figure 5.2

### 5.2.3 FRESNEL ZONE CALCULATION

To calculate the midpath obstacle loss it is necessary to draw the path profile for Fresnel zone. To design UHF link for Bangladesh it is considered that terrain the is flat with trees of about 15 m height on the average. To avoid intervening obstacles such a path profile is drawn in the fig.5.3.

### 5.2.4 PERFORMANCE CALCULATION

#### ANTENNA GAINS:

$$G_{dB} = 20\log(F) + 20\log(D) + 17.8 \quad [F \text{ in GHz, } D \text{ in meter}]$$

$$= 22.9 \text{ dB.}$$

#### PATH LOSS:

$$L_{dB} = 20\log(F) + 20\log(d) + 92.5 \quad [F \text{ in GHz, } d \text{ in km}]$$

$$= 123.98 \text{ dB.}$$

#### RECEIVER NOISE:

$$N_0(\text{dB}) = 10\log(KTB) + NF \quad [T = 318^0\text{k}]$$

$$= -102.13 \text{ dBm}$$

#### RECEIVER POWER:

$$P_r(\text{dB}) = 22.9 + 22.9 + 30 - 123.98 - (5.5 + 5.5) - 4.5$$

$$= -63.7 \text{ dBm.}$$

#### SIGNAL TO THERMAL NOISE RATIO:

$$(C/N)_{TH} = -63.7 - (-102.13)$$

$$= 38.43 \text{ dBm.}$$

5.2.5 A comparison for the specified results for 25 km UHF link shown in the table 5.01.

Table-5.01

	Receiving Antenna Height(h ) (m)	Antenna Gain (dB)	Path Loss (dB)	Receiver Input Power (dBm)
Calculated Values	22.00 (From First Lobe)	22.90	123.98	-63.70
Values Collected From T&T Board	24.00	23.40	123.90	-65.70

### 5.3 CALCULATION FOR A SHF LINK (Manikganj-Dhaka Radio Link)

This section deals with the performance calculation of Manikganj to Dhaka radio link. The diffraction loss and attenuation by atmospheric hydrometeors are consider negligible.

#### 5.3.1 Hop Characteristics

Hop Length .....44.30 km  
 Output Power .....30.00 dBm  
 Branching Losses..... 4.50 dB  
 Obstruction Losses ..... 6.00 dB

#### 5.3.2 Station Parameters:

Antenna Diameter ..... 3.70 m



Frequency Used ..... 6.77 GHz

Feeder Loss ..... 4.20 dB (Transmitting Side)  
 5.00 dB (Receiving Side)

Noise Figure ..... 3.00 dB

### 5.3.3 Results

[Coverage Diagram is shown in the Fig.5.5 and Fig.5.6]

Antenna Gain ..... 46.00 dB  
 Path Loss ..... 142.00 dB  
 Receiver Noise ..... -102.13 dBm  
 Received Power..... -33.70 dBm  
 (S/N)<sub>Th</sub>..... 68.13 dBm

5.3.4 A comparison between the calculated results and results calculated by Fujitsu Ltd. is shown in the table 5.02.

Table-5.02

	Path Loss ( dB )	Received Power ( dBm )	Antenna Gain ( dB )	Received Antenna Height(m)
Calculated Value	142.00	-33.70	46.00	61.00
Calculated by Fujitsu Ltd.	141.00	-34.25	45.7	63.00

### 5.4 DISCUSSIONS

The span length is very large compared to the antenna height and in above two cases the grazing angle is very small as

below one degree. Hence taking the reflection co-efficient taking -1 gives the accurate result of coverage diagram. The magnitude and phase of reflection co-efficient in 3-12 GHz range MW frequencies are shown in figures 5.7 and 5.8.

There is a thumb rule to determine the conditions under which the flat-earth formulas will serve a good results with acceptable accuracy. It is required that the flat-earth formula be accurate to within i,e  $(2k_0 h_1 h_2 / d - \lambda f v) < 0.15\lambda$ . In both cases it is not exactly satisfactory. Hence the spherical earth approximation is the exact solution for both the links.

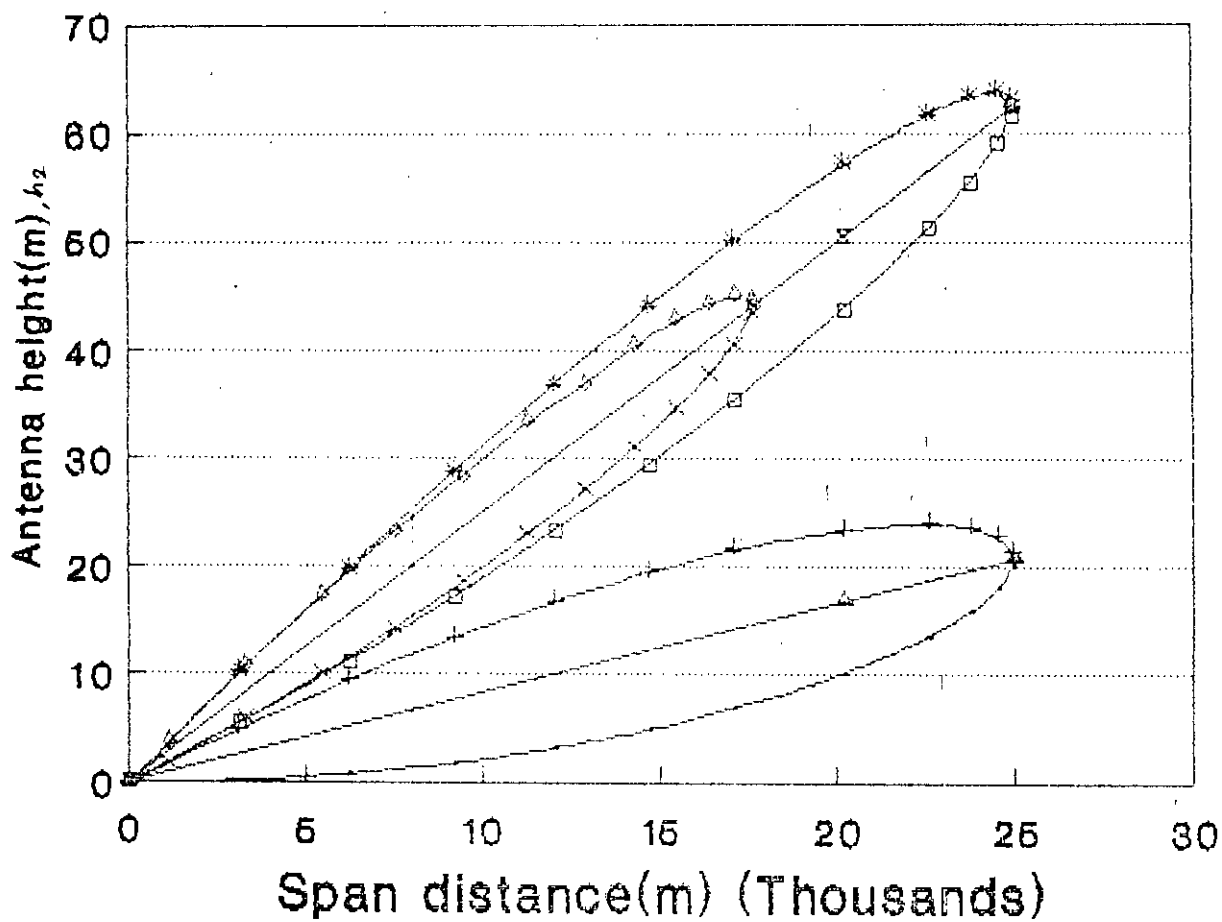


Fig.5.1 Coverage diagram (Flat earth approximation) for an UHF link ( $h_1=300\lambda_0$ ,  $r_f=12.5\text{Km}$ )

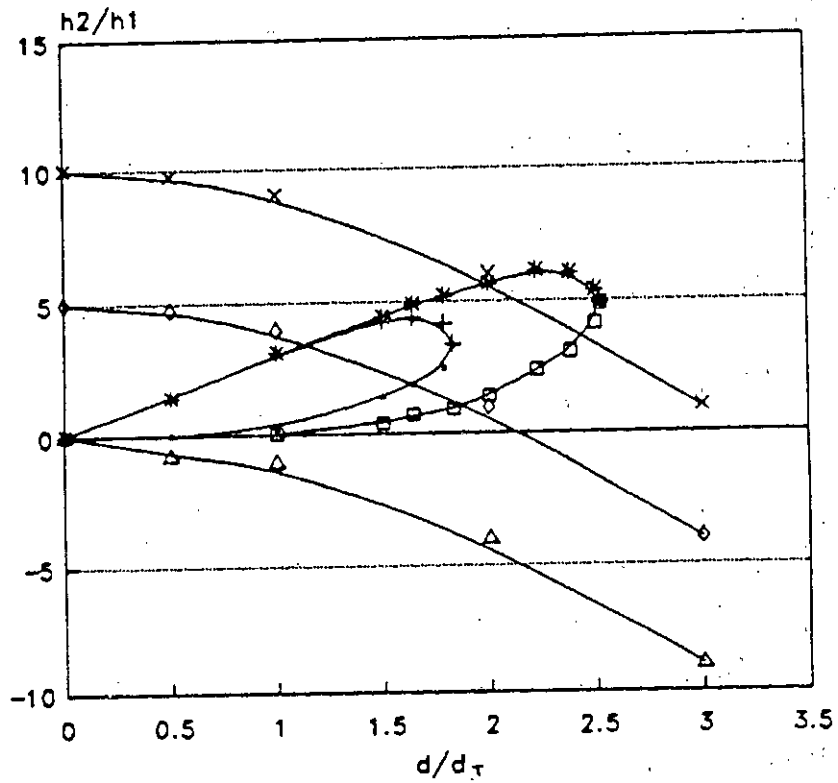


Fig.5.2 Coverage diagram (Spherical earth approximation) for an UHF link ( $v = 0.57$ )

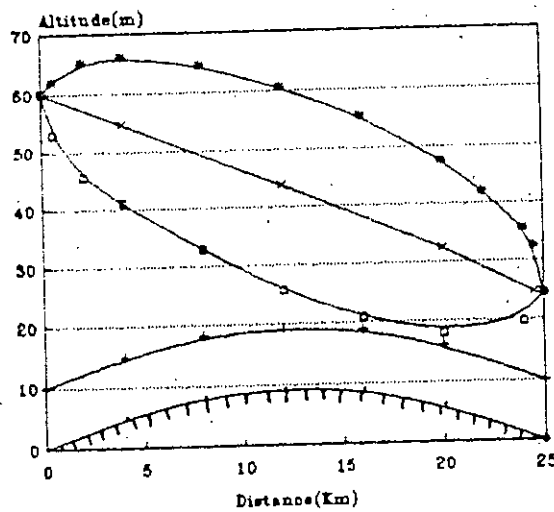


Fig.5.3 First Fresnel zone for an UHF link ( $f=1.5$  GHz,  $d=25.0$  Km,  $k=1.33$ ,  $h_1=24.0$  m,  $h_2=60.0$  m)

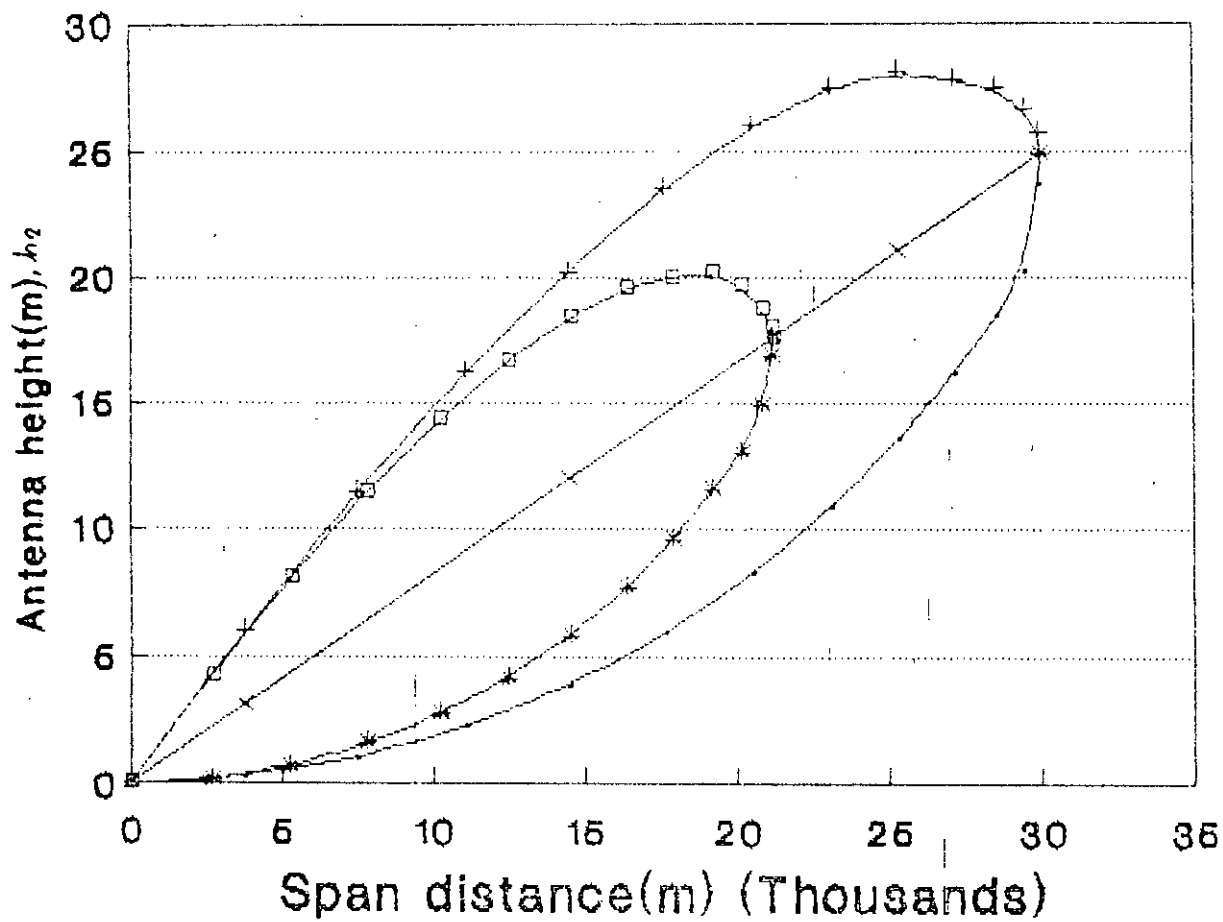


Fig. 5.4 Coverage diagram for an UHF link ( $h_1=300\lambda_0$ ,  $r_f=15\text{Km}$ )

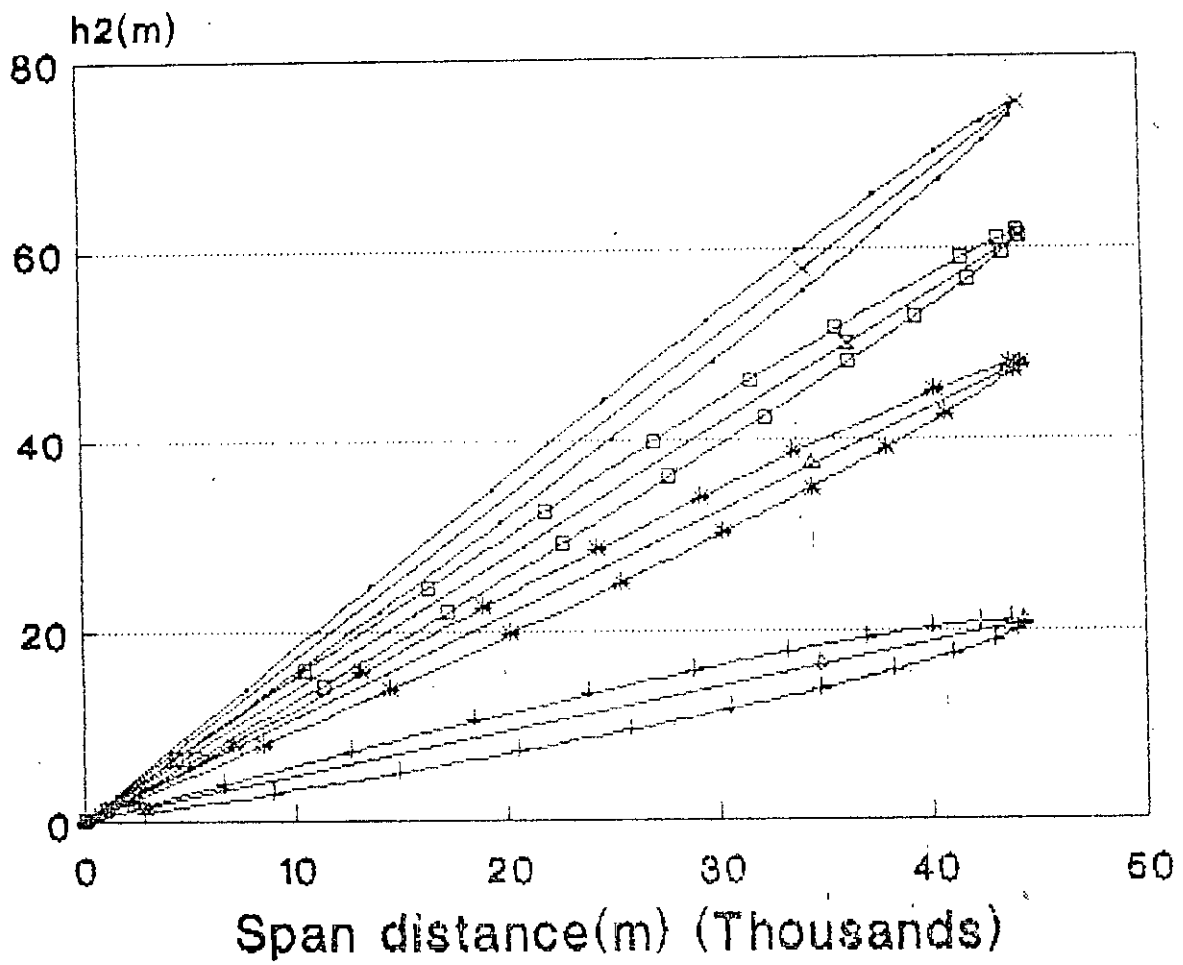
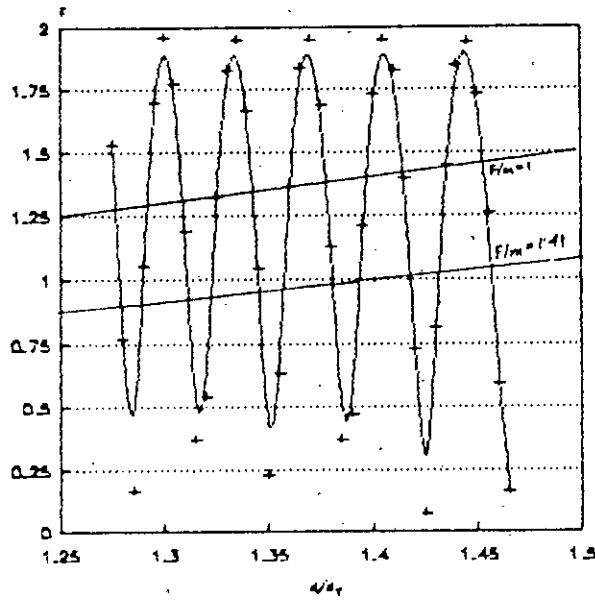
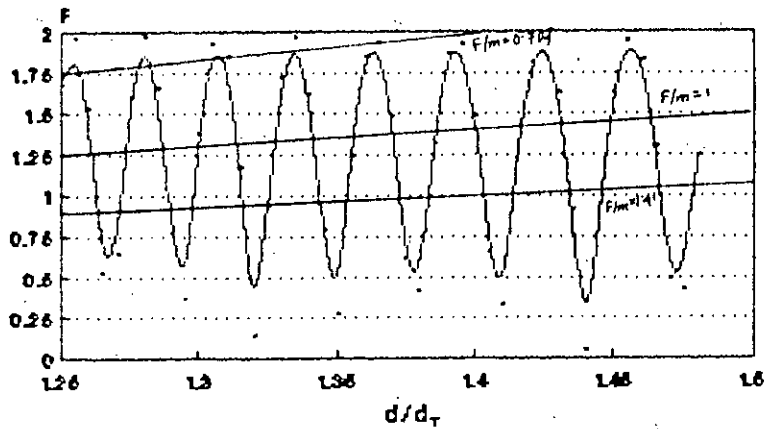


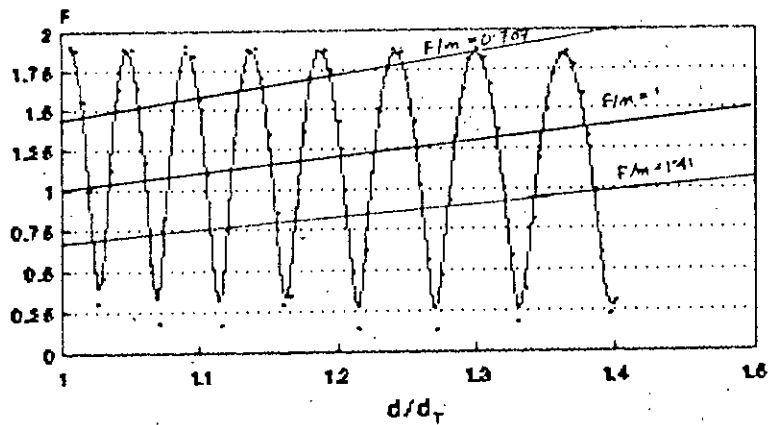
FIG.5.5 Coverage diagram for Manikganj-Dhaka mw link.  
 ( $h_1=86.0m$ ,  $f=6.77$  GHz,  $r_f=22.15$  Km)



$h_2/h_1 = 9$

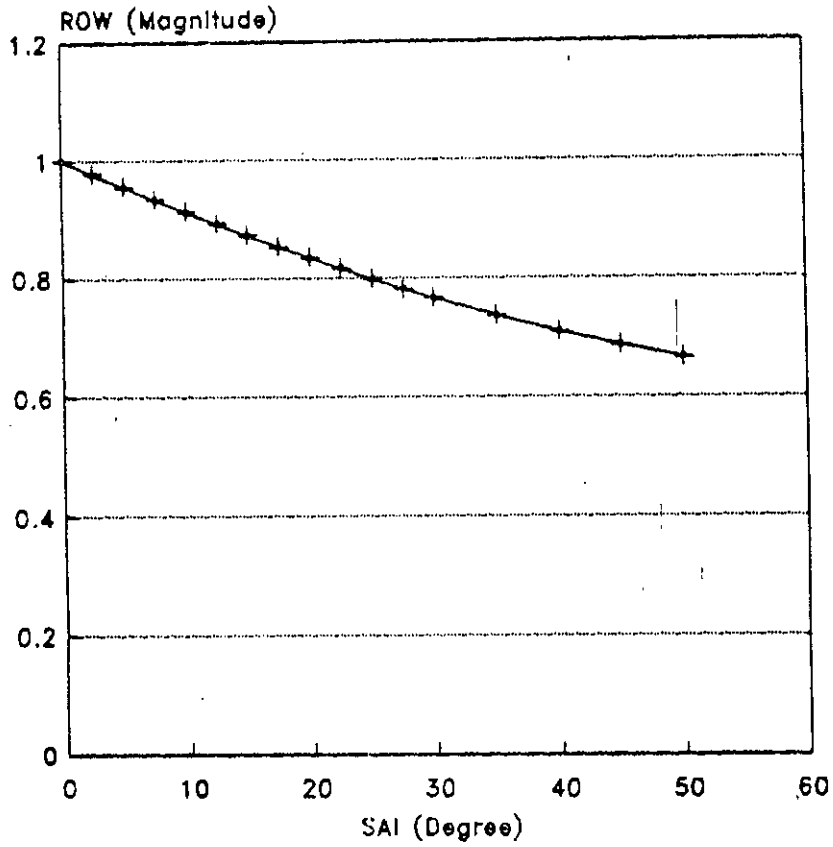


$h_2/h_1 = 6$

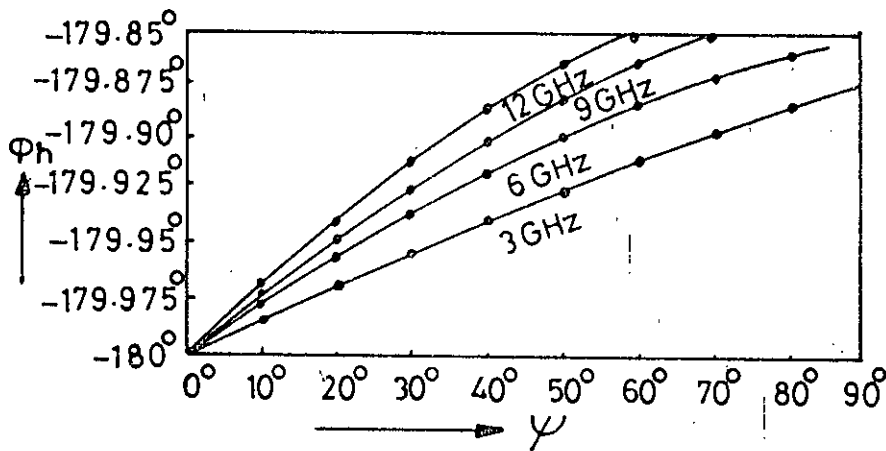


$h_2/h_1 = 2$

Fig. 5.6 Data for constructing coverage diagram for Manikganj-Dhaka MW link (Spherical earth) for  $v = 10.956$ .



(a)



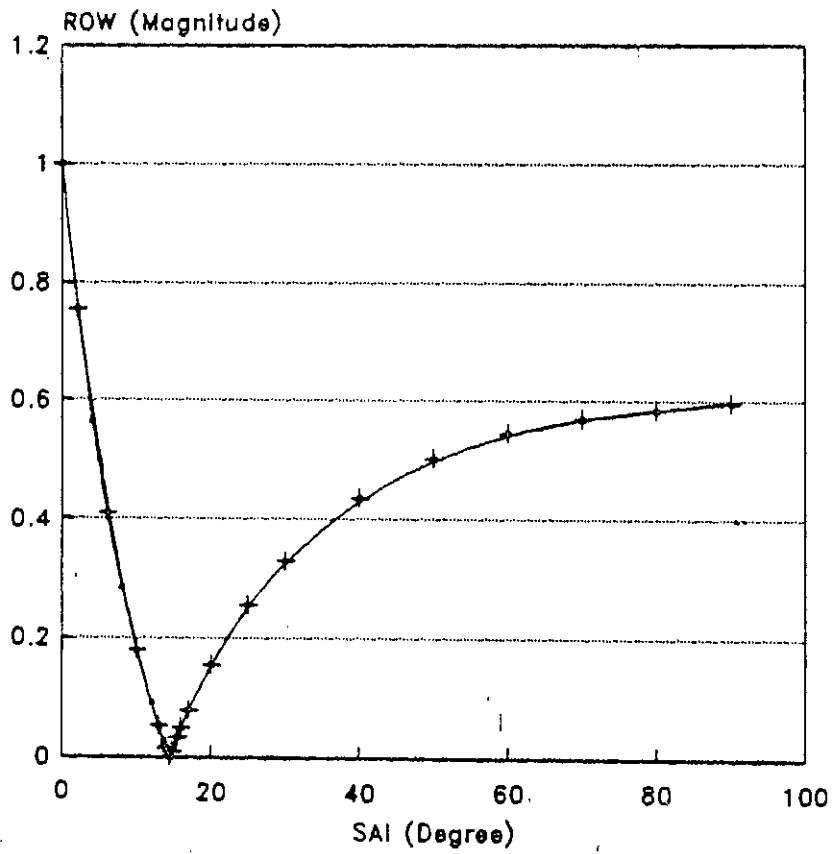
(b)

Fig. 5.7 Magnitude and phase of reflection co-efficient horizontal polarization in 3-12 GHz range ( $\epsilon = 15$ ;  $\sigma = 0.009$ )

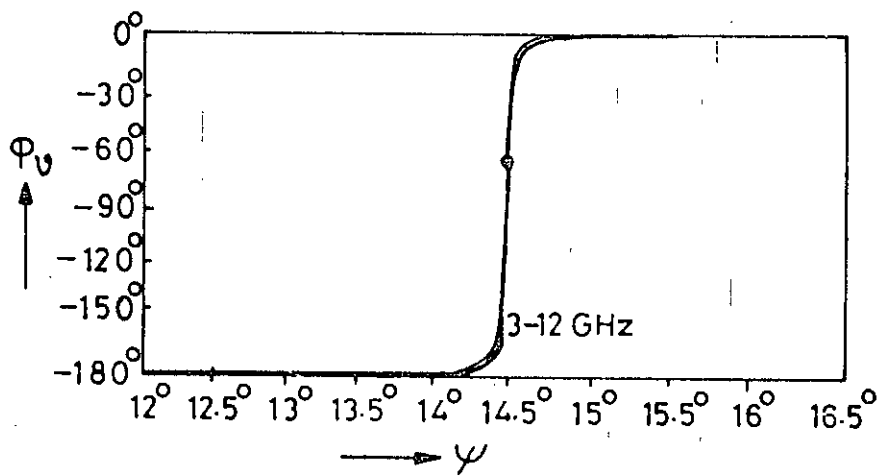
(a) Magnitude of the reflection coefficient

(b) Phase of the reflection coefficient





(a)



(b)

Fig. 5.8 Magnitude and phase of reflection co-efficient for vertical polarization in 3-12 GHz range ( $\epsilon = 15, \sigma = 0.009$ ).

- (a) Magnitude of reflection co-efficient
- (b) phase of reflection co-efficient

## CHAPTER 6

### CONCLUSIONS

#### 6.1- SUMMARY:

Throughout the thesis work the patterns of coverage diagram and the required field strength in the receiving side has been found by using the radio wave propagation phenomena over flat earth and spherical earth. To draw the patterns of coverage diagram and to find the field strength using flat-earth formula has been discussed in chapter two and the spherical earth phenomena has been discussed in chapter three. The performance calculation has been discussed in chapter four. Chapter five deals with the calculation for a number of microwave links in Bangladesh and the results are compared with the data taken from the Bangladesh T. & T. Board. The agreement between the two results is found to be satisfactory.

#### 6.2-SUGGESTION FOR FUTURE WORK:

At very high frequencies, several gigahertz and up, attenuation and scatter by rain and atmospheric gases, predominantly water vapor, must also be considered. Uncondensed water vapor and oxygen both have various absorption lines in the centimeter and millimeter wave regions. Consequently, there are frequencies where high attenuation occurs and which are separated

by windows or frequency bands where the attenuation is much lower. Figure 6.01 shows the attenuation by oxygen and water vapor (uncondensed) at 20<sup>0</sup>C at sea level. In those bands where the attenuation exceeds 10 dB/km the range over which communication can take place is severely restricted. By a proper choice of frequencies it is possible to achieve much less attenuation. For frequencies above 300 GHz the minimum attenuation is still large, 6 dB per kilometer, and places a great restriction on the application of millimeter and submillimeter-wave radiation for terrestrial line-of-sight paths. Scattering and diffraction of radio waves by hills, buildings, trees etc., is also much more pronounced at the higher frequencies (above several GHz and up). The present thesis work can be extended for the studies of above phenomena in several gigahertz and up.

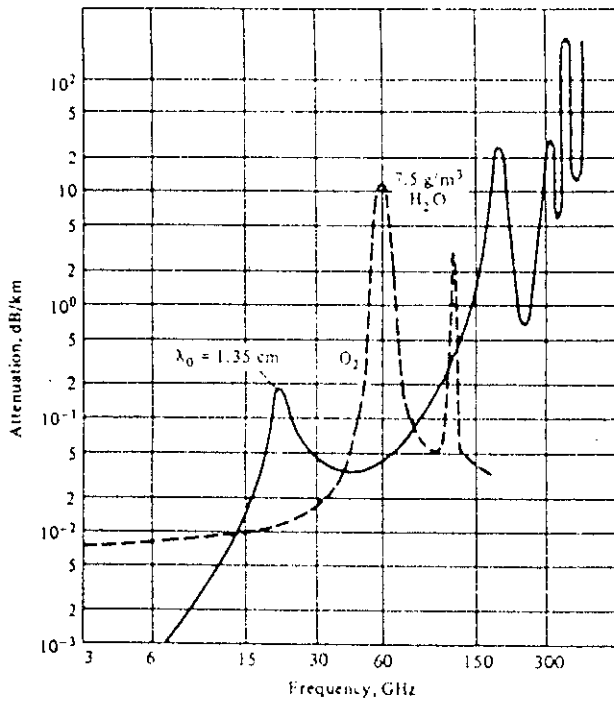


Fig. 6.1 Attenuation by oxygen and water vapor at sea level.  $T = 20^\circ\text{C}$ . ( This figure has been taken from reference 1 )

## APENDIX A

### MICROWAVE FREQUENCY BAND DESIGNATION \*\*\*\*\*

The range of microwave frequencies is broken down into several bands designated by letters is shown below:

<u>Frequency</u>	<u>Band designation</u>	
	OLD	NEW
500 - 1000 MHz	VHF	C
01 - 02 GHz	L	D
02 - 03 GHz	S	E
03 - 04 GHz	S	F
04 - 06 GHz	C	G
06 - 08 GHz	C	H
08 - 10 GHz	X	I
10 - 12.4 GHz	X	J
12.4 - 18 GHz	Ku	J
18 - 20 GHz	K	J
20 - 26.4 GHz	K	K
26.4 - 40 GHz	Ka	K

## APENDIX B

### CALCULATION OF (EFFECTIVE EARTH CORRECTION FACTOR) CONSTANT K

\*\*\*\*\*

From figure 3.03 we have

$$rd\theta = vdt \quad \dots\dots\dots(B.1)$$

$$\text{and } (r + dh)d\theta = (v + dv)dt \quad \dots\dots\dots(B.2)$$

Hence  $dhd\theta = dvdt$

$$\Rightarrow \frac{d\theta}{dt} = \frac{dv}{dh} \quad \dots\dots\dots(B.3)$$

But refractive index  $n = \frac{c}{v}$   
velocity in vacuum  
 $= \frac{\text{velocity in vacuum}}{\text{velocity in medium}}$   
 $= \frac{1/(\mu_0 k_0)^{1/2}}{1/(\mu k)^{1/2}}$   
 $= \left( \frac{\mu k}{\mu_0 k_0} \right)^{1/2}$

The permeability of troposphere and vacuum is same . Hence

$$n = (kr)^{1/2}$$

$$\Rightarrow (kr)^{1/2} = c/v = n$$

$$\Rightarrow v = c/n \quad \dots\dots\dots(B.4)$$

$$\Rightarrow dv/dh = -c/n^2 \cdot dn/dh$$

$$\Rightarrow dv/dn \cdot dn/dh = -c/n^2 \cdot dn/dh$$

$$\Rightarrow dv/dh = -(v/n) \cdot dn/dh$$

Since  $n$  is nearly equal to unity then we have

$$dv/dh = -v \cdot dn/dh \quad \dots\dots\dots(B.5)$$

From (B.1) we have

$$\begin{aligned} r &= v/(d\theta/dt) \\ &= v/(dv/dh) \quad \text{[Using (B.2)]} \\ &= -1/(dn/dh) \quad \text{[Using (B.5)]} \\ \Rightarrow 1/r &= -dn/dh \quad \dots\dots\dots(B.6) \end{aligned}$$

From figure 3.04a,

$$\begin{aligned} (a + h)^2 + d^2 &= (a + h + \delta h + x)^2 \\ \Rightarrow d^2 &= (x + \delta h)^2 + 2(a + h)(\delta h + x) \end{aligned}$$

But  $d \gg x$  or  $h$  &  $a \gg x$  or  $\delta h$ . Hence neglecting higher power of  $\delta h$

$$\begin{aligned} 2a(\delta h + x) &= d^2 \\ \Rightarrow \delta h &= \{d^2/(2a) - x\} \quad \dots\dots\dots(B.7) \end{aligned}$$

From figure 3.04a,

$$\begin{aligned} (a_e + h)^2 + d^2 &= (a_e + h + \delta h)^2 \\ \Rightarrow (\delta h)^2 + 2h\delta h + 2a_e\delta h &= d^2 \quad \text{[Neglecting higher power of } h] \end{aligned}$$

$$\begin{aligned} \Rightarrow \delta h &= d^2/2(a_e+h) \\ &= d^2/(2a_e) \quad \text{[As } a_e \gg h] \quad \dots\dots\dots(B.8) \end{aligned}$$

But from figure 3.04a,

$$r^2 + d^2 = (r + x)^2$$

$$\Rightarrow d^2 = 2rx \quad [ \text{As } r \gg x ]$$

$$\Rightarrow x = d^2/(2r) \quad \dots\dots\dots(B.9)$$

Hence using (B.7) & (B.9) we have

$$\delta h = (d^2/2)(1/a - 1/r) \quad \dots\dots\dots(B.10)$$

Equating (B.8) & (B.10)

$$\begin{aligned} 1/a_e &= 1/a - 1/r \\ &= 1/a + dn/dh \quad [\text{Using (B.6)}] \dots(B.11) \end{aligned}$$

Now we can put  $a_e = ka$  where  $k$  is the correction factor. Then we have

$$1/k = 1 + a \cdot dn/dh$$

$$\Rightarrow k = \frac{1}{1 + a \cdot dn/dh} \quad \dots\dots\dots(B.12)$$

The gradient of refractive index ( $dn/dh$ ) corresponding to standard atmospheric conditions is  $- 0.039 \times 10^{-6}$  per meter and the radius of earth ( $a$ ) is 6372 km.

Hence  $k = 1/(1 - 6372 \times 10^3 \times 0.039 \times 10^{-6})$   
 $\cong 4/3.$



## APPENDIX C

### LISTING OF COMPUTER PROGRAM \*\*\*\*\*

```

C   PROGRAM FOR THE CALCULATION OF COVERAGE DIAGRAM
C   FLAT-EARTH PHENOMENA FOR 30KM LINK
C
  OPEN(UNIT=1,STATUS='OLD',FILE='INPUT')
  OPEN(UNIT=2,STATUS='NEW',FILE='OUTPUT')
  READ(1,3) ALMDA, H1
3   FORMAT(3F10.3)
  WRITE(2,4) ALMDA, H1
4   FORMAT(3X,'ALMDA=',F10.3,3X,'H1='F10.3)
  PI=3.14159
  'FR' IS USED HERE FOR THE RATIO OF PATH GAIN FACTOR WITH 'R'
C
C   AO=2*PI/ALMDA
  DO 60 FRR = 1, 8, 1
  FR=FRR/15000
  HD=RECEIVING ANTENNA HEIGHT DIVIDED BY DISTANT
C
C   DO 50 DH = 1, 200, 1
  HD=DH/15000
  F=2*ABS(SIN(AO*H1*HD))
  R=F*15000/FRR
  DSTANT=((HD*H1)+((HD**2*H1**2)+(1+HD**2)*(R**2-H1**2))**0.5)/
+ (1+HD**2)
  HT=HD*DSTANT
  WRITE(2,5) FRR, F, DSTANT, HT
5   FORMAT(2X,'FRR=',F10.3,2X,'F=',F8.5,2X,'DSTANT=',F8.1,2X,
+ 'HT=',F6.2)
50  CONTINUE
60  CONTINUE
  STOP
  END

C
C   REFLECTION CO-EFFICIENT CALCULATION
C
  COMPLEX C,TT
  OPEN(UNIT=1,STATUS='OLD',FILE='INPUT')
  OPEN(UNIT=2,STATUS='NEW',FILE='OUTPUT')

```

```

      READ(1,3) AK, E1, SIGMA
3   FORMAT(3F10.3)
      WRITE(2,4) AK, E1, SIGMA
4   FORMAT(3X, 'AK=', F10.3, 3X, 'E1=', F10.3, 3X, 'SIGMA=' F10.3)
      PI=3.14159
      DO 60 FRQ = 3, 12, 3
      DO 50 SAI =0, 360, 1
      FREQ=FRQ/2
      SI=SAI*PI/720
      SAI1=SAI/4
      AX=18*SIGMA/FREQ
      X1=-ABS((COS(SI))**2)+AK
      Y1=-AX
      C=CMPLX(X1,Y1)
      TT=CSQRT(C)
      X2=REAL(TT)
      Y2=AIMAG(TT)
      X3=AK*ABS(SIN(SI))
      Y3=Y1*ABS(SIN(SI))
      TAI1=X3-X2
      PAI1=Y3-Y2
      TAI2=X3+X2
      PAI2=Y3+Y2
      TAI=SIN(SI)-X2
      PAI=-Y2
      TA2=SIN(SI)+X2
      PA2=Y2
      RW1=((TAI1**2+PAI1**2)/(TAI2**2+PAI**2))**0.5
      XX=PAI1/TAI1
      YY=PAI2/TAI2
      FII1=((ATAN(XX)-ATAN(YY))*180)/PI
      RW2=((TAI**2+PAI**2)/(TA2**2+PA2**2))**0.5
      WW=PAI/TAI
      ZZ=PA2/TA2
      FII2=((ATAN(WW)-ATAN(ZZ))*180)/PI
      WRITE(2,5) RW1, RW2, SAI1, FII1, FII2, AX
5   FORMAT(2X, 'RW=', F9.5, 1X, 'RW2=', F9.5, 1X, 'SAI1=', F5.2, 1X,
+ 'FII1=', F10.5, /1X, 'FII2=' F10.5, 1X, 'AX=' F15.5)
50  CONTINUE
60  CONTINUE
      STOP
      END

```

C  
C THIS SAME PROGRAM CAN BE USED FOR CALCULATION REFLECTION  
C CO-EFFICIENT AT DIFFERENT PARAMETERS .

C  
C AVAILABLE DATA FOR THE INTERFERENCE PATTERNS OF MW LINK IN  
C CASE OF SPHERICAL EARTH (DHAKA TO MANIKGANJ)  
C

```

OPEN(UNIT=1,STATUS='OLD',FILE='INPUT')
OPEN(UNIT=2,STATUS='NEW',FILE='OUTPUT')
READ(1,3) H1, FREQ
3  FORMAT(2F10.3)
WRITE(2,4) H1, FREQ
4  FORMAT(3X,'H1=',F10.3,3X,'FREQ=',F10.3)
PI=3.14159
ALAMDA=GREECK LAMDA, DSTNT=SPAN LENGTH,HH=H2/H1,DDT=DSTNT/DT

ALMDA=0.3/FREQ
V=(H1**1.5)/(1030*ALMDA)
DT=4120*H1**0.5
C THIS LOOP IS USED FOR CALCULATION PARAMETERS WITH INCREASING
C RECEIVING ANTENNA HEIGHT.
DO 40 H2 =63, 1000, 126
HADD =H1+H2
HMNUS=H1-H2
T=(H1/H2)**0.5
HH=1/T**2
C THIS LOOP IS USED FOR CALCULATION PARAMETERS WITH INCREASING
C DISTANCE
DO 24 DD =25, 400, 1
DDT=DD/200
DSTNT=DT*DDT
P=((2*(4120**2)*HADD+DSTNT**2)/3)**0.5
SAI=ACOS((4120**2*HMNUS*DSTNT)/P**3)
D1=DSTNT/2+P*COS((SAI+PI)/3)
D2=DSTNT-D1
SI=D1/DT
S2=D2/(4120*H2**0.5)
S=(S1*T+S2)/(1+T)
D=1/(1+(4*S1*S2**2*T)/(S*(1-S2**2)*(1+T)))*0.5
GTA=HH*(1-S1**2)*(1-S2**2)/DDT

```

```

      F=((1+D)**2-4*D*(COS((PI*V*GTA)/2)**2))**0.5
      FDDT=DDT/F
      YH=HH-DDT**2
      WRITE(2,5) HH, DDT, DSTNT, F, GTA, D, YH
5     FORMAT(1X, 'HH=', F4.1, 1X, 'DDT=', F6.3, 1X, 'DSTNT=', F10.2, 1X,
+ 'F=', F8.5, 1X, 'GTA=', F8.5, 1X, 'D=', F7.5, 1X, 'YH=', F8.5)
24    CONINUE
40    CONTINUE
      STOP
      END

```

## References

- [1] Robert E. Collin,- 'Antennas and Radiowave Propagation' Case Western Reserve University, McGraw-Hill Book Company, 1987, pp.303-333 and 339-377.
- [2] S. Ramo and J.R. Whinnery,-'Fields and Waves in Modern Radio' 2nd edd., John Wiley and Sons, Inc., New York, 1953, pp. 150-160.
- [3] J. E. Flood,-'Telecommunication Networks', Peter Peregrinus Ltd. IEE England, 1977, pp.33-38.
- [4] George Kennedy,- 'Electronic Communication System' Second Edition, McGraw Hill International Book Company. 1981, pp.10-16, 22-27 and 248-275.
- [5] E. C. Jordan and K. G. Balmain,-'Electromagnetic waves and Radiating System', Prentice Hall, Inc, Englewood, New Jersey. 1968, pp. 628-681.
- [6] M. L. Sony and J. C. Gupta,- 'A Course in Electronic & Communication Enginnering'- Dhanpat Rai & Sons, 1682-NAI Sarak, Delhi-110006, pp. 1071-1105.
- [7] J. A. Saxton,-'Radio wave Propagation in the Troposphere' Elsevier Publishing Company, New York, 1962.
- [8] Kamilo Feher, - 'Digital Communications ( Microwave applications )', Prentice Hall Inc., Englewood Cliffs, New Jersey, pp. 94-102.
- [9] I. H. Gerks, -'Factors Affecting Spacing of Radio terminals in UHF Link', Proc. IRE, 43, No. 10, Oct. 1955, pp.1290-1297.

- [10] W. E. Gordon, - 'Radio Scattering in the Troposphere'  
Proc. IRE, 43, Jan. 1955, pp. 23-28.
- [11] Sanjeeva Gupta, - 'electronics communications'  
Khanna Publishers, 2-B Nath Market, Nai Sarak, Delhi, 1988,  
pp. 5-25 and 211-256.
- [12] B. R. Bean and F. M. Meaney, - 'Some Applications of the  
Monthly Median Refractivity Gradient in Tropospheric  
Propagation', Proc. IRE, 43, Oct. 1955, pp. 1419-1431.
- [13] K. A. Norton, - 'The Propagation of Radio waves over the  
Surface of the Earth', Proc. IRE, 24, 1936, pp.1364-1365.
- [14] J. R. Carson, - 'Reciprocal Theorems in Radio Communications'  
Proc. IRE, Vol. 17, No. 6, 1929, pp. 252-253.
- [15] D. E. Kerr, - 'Propagation of Short Radio Waves'  
McGraw-Hill Book Company, New York, 1951, pp. 40-66.
- [16] W. L. Flock and E. K. Smith, - 'Natural Radio Noise- A mini  
Review', IEEE Trans., Vol. AP-32, July 1984, pp. 762-767.
- [17] K. Bullington, - 'Radio Propagation at Frequencies above 30  
Megacycles', Proc. IRE, Vol. 35, 1947, pp. 1120-1124.
- [18] F. E. Terman, - 'Electronic and Radio Engineering', 4th edd.  
McGraw- Hill Book Company, New York, 1955, pp. 803-863.

